

UNCLASSIFIED

AD 408 704

DEFENSE DOCUMENTATION CENTER

FOR

SCIENTIFIC AND TECHNICAL INFORMATION

CAMERON STATION, ALEXANDRIA, VIRGINIA



UNCLASSIFIED

NOTICE: When government or other drawings, specifications or other data are used for any purposes other than in connection with a definitely related government procurement operation, the U. S. Government thereby incurs no responsibility, nor any obligation whatsoever; and the fact that the Government may have formulated, furnished, or in any way supplied the said drawings, specifications, or other data is not to be regarded by implication or otherwise as in any manner licensing the holder or any other person or corporation, or conveying any rights or permission to manufacture, use or sell any patented invention that may in any way be related thereto.

63 4-2

ASD-TDR-62-186
PART II

CATALOGED BY DDC
AS AD No. 108704

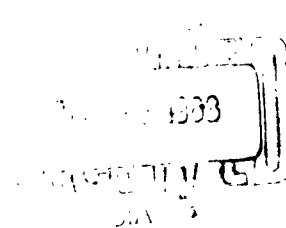
408 704

ULTRASONIC METHODS IN THE STUDY OF FATIGUE AND DEFORMATION IN SINGLE CRYSTALS

TECHNICAL DOCUMENTARY REPORT ASD-TDR-62-186 PART II

April 1963

Directorate of Materials and Processes
Aeronautical Systems Division
Air Force Systems Command
Wright-Patterson Air Force Base, Ohio



Project No. 7360, Task No. 736002

(Prepared under Contract No. AF 33(657)-8324 by
Brown University, Providence, R. I.;
Bruce Chick, Akira Hikata, George Anderson, William Findley,
Charles Elbaum, Rohn Truell, authors)

NOTICES

When Government drawings, specifications, or other data are used for any purpose other than in connection with a definitely related Government procurement operation, the United States Government thereby incurs no responsibility nor any obligation whatsoever; and the fact that the Government may have formulated, furnished, or in any way supplied the said drawings, specifications, or other data, is not to be regarded by implication or otherwise as in any manner licensing the holder or any other person or corporation, or conveying any rights or permission to manufacture, use, or sell any patented invention that may in any way be related thereto.

Qualified requesters may obtain copies of this report from the Armed Services Technical Information Agency, (ASTIA), Arlington Hall Station, Arlington 12, Virginia.

This report has been released to the Office of Technical Services, U.S. Department of Commerce, Washington 25, D.C., in stock quantities for sale to the general public.

Copies of this report should not be returned to the Aeronautical Systems Division unless return is required by security considerations, contractual obligations, or notice on a specific document.

ASD TDR 62-186
PART II

ULTRASONIC METHODS IN THE STUDY OF FATIGUE
AND DEFORMATION IN SINGLE CRYSTALS

1 APRIL 1963

Directorate of Materials and Processes
Aeronautical Systems Division
Air Force Systems Command
Wright-Patterson Air Force Base, Ohio

Project No. 7360, Task No. 736002

(Prepared under Contract No. AF 33(657)-8324
by the Metals Research Laboratory, Brown University, Providence, R. I.;
Bruce Chick, Akira Hikata, George Anderson, William Findley
Charles Elbaum, Rohn Truell, authors)

FOREWORD

This report was prepared by the Metals Research Laboratory, Division of Applied Mathematics, Brown University, Providence, Rhode Island under USAF Contract No. AF33(657)-8324. The contract was initiated under Project No. 7360, "The Chemistry and Physics of Materials", Task No. 736002, "Nondestructive Methods." The work was administered under the direction of the Directorate of Materials and Processes, Deputy for Technology, Aeronautical Systems Division, with Mr. W. L. Shelton acting as the project engineer.

This report covers work conducted from February 1, 1962 to February 1, 1963, and is a continuation of work done under Contract No. AF 33(616)-6945.

We are indebted to Mr. Richard Rowand for direct assistance and for encouragement in connection with this work.

ABSTRACT

The use of ultrasonic methods (and in some cases electrical conductivity measurements) for studying defect formation and motion in connection with deformation and stress cycling experiments in aluminum and sodium chloride single crystals is the subject of this report.

Previous work has shown that the observed ultrasonic changes are closely associated with changes in dislocation behavior. It was shown that it was possible to use deformation experiments in such a way that the results could be related to the action of the slip systems and to their orientation. It was shown that dislocation breakaway, easy glide, and dislocation multiplication were indicated by attenuation and velocity changes.

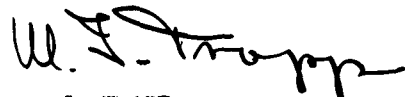
Measurements on large single crystals of sodium chloride, deformed in tension, have been made in a manner similar to that with aluminum for the purpose of comparing the dislocation damping and recovery effects in an ionic crystal with those in a metal. In addition there is significant information from electrical conductivity measurements made concurrently with attenuation and velocity measurements.

Recovery in aluminum single crystals at 195°K has been compared with recovery at room temperature with the result that an interesting "threshold effect" has been observed; there appears to be a level of deformation which must be exceeded, at this temperature before recovery occurs.

Stress cycling experiments on aluminum single crystals cycled in tension and compression have shown some interesting consequences in comparison with our earlier results on polycrystalline samples. Single crystals (high purity) can be cycled at levels much higher relative to yield stress and breaking stress than can polycrystalline (commercial purity) samples at the same time the stress level can be raised in steps during cycling until it is one and a half to two times (at least) the stress that would be required initially to break the single crystal sample.

The automatic recording time echo (or velocity) measurement unit has been designed to measure the time between two successive echoes in a pulse echo train with a sensitivity of one nanosecond out of one hundred microseconds and to record the measurement as a voltage capable of driving a recorder so that dynamic changes in time (that cannot be measured manually) will produce a record. The system must be independent of variations in repetition rate, and time jitter, and change in amplitude of the echoes selected. These aims have been accomplished in the trial model of this device. In particular it has been found that no change in center frequency or bandwidth is seen over a 40 db range of gain control nor does an artificial change of 40 db in signal level produce a detectable change in measured time.

This technical documentary report has been reviewed and is approved.



W. J. TRAPP
Chief, Strength & Dynamics Branch
Metals and Ceramics Division
Air Force Materials Laboratory

TABLE OF CONTENTS

SECTION	PAGE
Introduction	1
Recovery of Aluminum	
Discussion of measurements and results concerned with the recovery after deformation of aluminum single crystals at room temperature and at 195°K as well as conditions for deformation with no recovery	3
Anomalous Velocity Effect	12
Deformation in Ionic Crystals (NaCl, LiF)	
Ultrasonic attenuation and velocity changes associated with dislocation motion during deformation. Conductivity or charge effects arising from dislocation motion during deformation.	29
Stress Cycling of Single Crystal Aluminum	
Ultrasonic changes and stress-strain changes as a function of cycling for about 3×10^6 cycles.	59
Automatic Recording Velocity Measurement Unit	70
References	75

INTRODUCTION

The purpose of this investigation is that of understanding the physical changes which are detected and continuously measured in aluminum and in certain ionic crystals during deformation and stress cycling. The investigation involves the study of imperfection behavior generally, and specifically the interaction of point defects with moving and vibrating dislocations. The study of metals and ionic crystals offers information specific to these two types of materials as well as information on imperfection behavior in general.

Previous work has been concerned with aluminum single crystals oriented for single slip and for "polyslip" deformed in tension, at room temperature. Simultaneous measurements of attenuation and velocity changes were made continuously during tensile deformation. The observed changes in attenuation in the polyslip orientations are consistent with an explanation based on the number of equally favored slip systems in each case. The results on crystals oriented for single slip indicate that in the easy glide range of strain hardening, dislocation multiplication is confined to the primary slip system only. The end of easy glide is associated with dislocations multiplying in other slip systems. An increase in attenuation is also observed prior to the onset of the macroscopic yield. This increase is attributed to an increase in dislocation loop length, caused by a breakaway mechanism.

In the early stages of deformation, for all orientations, an increase of ultrasonic velocity, relative to the unstrained condition, is observed. This initial increase in velocity is discussed under the "anomalous velocity effect" and the effect forms one of the strongest tests of dislocation damping theory. Similar deformation experiments have been carried out on sodium chloride single crystals.

During the past year we have extended this work in the direction of studying the charge distribution and conductivity in alkali halides and the association of these

Manuscript released by the authors 1 April 1963 for publication as an ASD Technical Documentary Report.

properties with plastic deformation. More specifically, we have studied the charge transported by moving dislocations during plastic strain as well as the conductivity change at different temperatures associated with plastic deformation in alkali halides. In addition to conductivity measurements the changes in the material are detected and followed by the measurement of ultrasonic attenuation and velocity using pulse echo methods in the low megacycle range of frequencies. A discussion of our earlier work is given together with further references, in our annual report, dated February, 1962, entitled "Ultrasonic Methods in the Study of Fatigue and Deformation in Single Crystals" Technical Documentary Report No. ASD-TDR-62-186.

The present report is concerned with the following topics:

1. Discussion of measurements and results concerned with the recovery after deformation of aluminum single crystals at room temperature and at 195°K as well as conditions for deformation with no recovery.

2. Anomalous Velocity Effect.

3. Deformation in Ionic Crystals (NaCl, LiF)

Ultrasonic attenuation and velocity changes associated with dislocation motion during deformation. Conductivity or charge effects arising from dislocation motion during deformation.

4. Stress Cycling of Single Crystal Aluminum

Ultrasonic changes and stress-strain changes as a function of cycling for about 3×10^6 cycles.

5. Automatic Recording Velocity Measurement Unit.

It should be noted that each of the above mentioned sections can stand by itself, and that the figures are numbered consistently within each individual section.

1. Recovery of Aluminum

Recovery of aluminum (and other solids), following deformation, is observed in both attenuation and velocity measured as a function of time until the attenuation has dropped (or the velocity increased) to a steady value. The final value may be the same as the initial value of attenuation (or velocity) before deformation. In other words the attenuation may recover completely or partially toward the initial value before deformation.

The recovery process is one in which the dislocations are repinned (the loop lengths shortened) by the point defects which migrate to the dislocations as a function of time after the deformation has been stopped. The recovery process will proceed whether or not the load is removed. At room temperature the recovery will proceed rapidly as soon as the loading is stopped. Of course some recovery is present during the loading process, and if the loading is done very slowly the recovery may nearly cancel the unpinning process.

The manner in which this repinning occurs is sensitive to the conditions under which the point defects must operate. Recovery is sensitive to temperature, to purity, to dislocation density, to types of dislocation and so on. Recovery measurements should also reveal whether more than one type of point defect is involved in the recovery process. Study of recovery may allow a determination of the period of time, during the pinning process, for which the diffusion of point defects limits or determines the rate of recovery. Recovery measurements at low temperatures, when compared with similar measurements at room temperature, will reveal whether a particular point defect is sufficiently active at various temperatures to cause pinning and in this way may help to identify what point defect is under examination. With two (or more) types of point defects involved in pinning it should be possible to separate the effects of each type by doing recovery experiments at several different temperatures

including a temperature which "stops" one defect and leaves the other active, and finally at a temperature which "stops" the second defect also. This may, of course, not be possible, but if it is, one can hope to find out what the defects are and how many types are involved.

With such ideas in mind we have examined the recovery of pure aluminum single crystals at room temperature and at 195°K with the intention of continuing at lower temperatures.

Several results of interest have emerged. The recovery behavior has been shown to obey the $t^{2/3}$ law rather well during the first stages of (30 minutes) recovery. An interesting "plateau" appears in the recovery curve at low temperatures but not at room temperature. In addition it has been found that there is a threshold in the deformation below which recovery does not occur at all at the lower temperature.

Figure 1 shows a room temperature recovery curve (with load removed) for comparison with the recovery curve of Figure 2 taken at 195°K. The data of Figure 2 show the plateau mentioned above; the plateau has always appeared as shown with aluminum, and it may be noted that a very similar effect appears when sodium chloride is irradiated at 77°K with Co^{60} gamma rays.

Dislocation damping theory shows that the attenuation should depend on loop length (average) L , dislocation density Λ , and ultrasonic frequency ν , $\omega = 2\pi\nu$ in the following way

$$\alpha = K_1 \omega^2 \Lambda L^4 \quad \text{db}/\mu \text{ sec}$$

where

$$K_1 = 8.68 \times 10^{-6} \left(\frac{4Gb^2}{\pi^4 c} \right) \left(\frac{B}{\pi^2 c} \right)$$

The dislocation loop length should decrease during recovery and the decrease in loop length should depend on the concentration of effective pinning agents $c(t)$ added during recovery to the initial average loop length L_0 . Then the loop length at any

time t after recovery begins will be $L = \frac{L_0}{1 + c(t)}$

From arguments involving the diffusion of point defects it can be deduced that the concentration of pinning points $c(t) = \beta t^{2/3}$ where $\beta = \text{constant} \left(\frac{AD}{kT} \right)^{2/3}$ where A is a factor indicating the strength of the Cottrell attraction between dislocations and point defects. Using $c(t) = \beta t^{2/3}$ leads to

$$\alpha = K_1 \omega^2 \Lambda L_0^4 \frac{1}{[1 + \beta t^{2/3}]^4}$$

ω , Λ , and L_0 are regarded as fixed quantities during recovery and we normalize to $K_1 \omega^2 \Lambda L_0^4$ hence $\alpha_n = \frac{1}{[1 + \beta t^{2/3}]^4}$ and from this it is evident that

$$[\alpha_n^{-1/4} - 1] = \beta t^{2/3}$$

Using the data of Figure 2, $[\alpha_n^{-1/4} - 1]$ is plotted as a function of $t^{2/3}$ in Figure 3 where it is seen that the relation is a linear one. The value of β obtained at 195°K from Figure 3 is $0.12 (\text{min})^{-2/3}$. The ultrasonic frequency used in these frequencies was 20mc/sec and the purity of the aluminum was about 99.998%.

The interest in values of β arises from the fact that activation energies for motion of the relevant point defects can be found from plots of $\log \beta$ as a function of $\frac{1}{kT}$ because these curves should be straight lines with slope equal to $(2/3)U$ where U is the activation energy for the migration of the point defect effective in the pinning process. If β is evaluated at two temperatures T_1 and T_2 it can be shown that the activation energy U may be obtained from the expression

$$U = \frac{\log_e \left(\frac{\beta(T_1)}{\beta(T_2)} \right)}{\frac{2}{3k} \left(\frac{1}{T_2} - \frac{1}{T_1} \right)}$$

Measurements of this type have been made at 195°K and at 295°K. There are, however, difficulties which we have encountered in interpreting the results of these

measurements because the activation energies obtained are unexpectedly small. The values are such (order of 0.05 ev.) that they are only two or three times the value of kT at 200°K , and the meaning of an activation energy under such circumstances would be questionable. Although the plot of Figure 3 fits the predicted linear relation with time very well for a period of about 30 minutes there may be difficulties with the temperature dependence. The derivation of the temperature dependence of β may be more complicated than that which we have used. This matter remains to be studied.

It was pointed out above that a rather surprising threshold effect was found in connection with the recovery experiments at 195°K . In particular it was found, for example, that a single crystal at 195°K had an attenuation of $0.104 \text{ db}/\mu \text{ sec}$ before deformation, and that after small deformation the attenuation increased to $0.138 \text{ db}/\mu \text{ sec}$ where it remained constant for ten minutes or more (i.e., no recovery).

Following this period in which no recovery in attenuation could be observed the sample was again deformed, and the attenuation increased from $0.138 \text{ db}/\mu \text{ sec}$ to $0.225 \text{ db}/\mu \text{ sec}$ which is obviously more than double the initial value of $0.104 \text{ db}/\mu \text{ sec}$. Again no recovery was observed for a period of nine to ten minutes at which time the load was removed; there was still no change in attenuation or any suggestion of recovery, and the attenuation value remained at $0.225 \text{ db}/\mu \text{ sec}$. The sample was next loaded and deformed a third time; the attenuation went to $0.305 \text{ db}/\mu \text{ sec}$ and this time recovery did occur. After 4 minutes (with load on) the attenuation recovered to $0.278 \text{ db}/\mu \text{ sec}$, and the sample was unloaded - during unloading the attenuation rose slightly to $0.290 \text{ db}/\mu \text{ sec}$ and decreased in less than an hour to $0.21 \text{ db}/\mu \text{ sec}$. After an additional five hours time the value remained unchanged at $0.21 \text{ db}/\mu \text{ sec}$. Figure 4(a) shows a rough plot of the events (in attenuation) just described.

A second recovery experiment of the same type (also at 195°K) showed the same features as the one just described (Figure 4b) except that in this second case echo time (velocity) measurements were made together with the attenuation measurements. In each case where the attenuation increased during loading the echo time increased as well (velocity decreased) and in each case where recovery occurred the velocity also recovered. In those cases where the attenuation did not recover the velocity also did not recover. In other words the velocity behaved as expected for a dislocation change.

As to why the attenuation recovery does not occur at 195°K with small deformation it appears that there is a range of deformation in which either the point defects necessary for repinning are not produced or released in sufficient numbers or they are produced and are not mobile at this temperature. The latter supposition seems unlikely, however, since with sufficient deformation recovery does occur. We do not know at present whether this threshold of strain for recovery has a temperature dependence or not. It is possible that there are at least two types of defects involved. If one of these two types of point defects is not mobile at this temperature and the second type is mobile then it is only necessary to suppose that the weaker pinning is provided by the non-mobile defect and that the dislocation breaks away from this weaker pinning first for small deformation; the non-mobile defect cannot repin. When the deformation is sufficient to break away from the stronger pinning, thereby releasing the relatively more mobile point defects, repinning can occur. Another possibility is that the defects capable of pinning are produced by dislocation intersections after a certain threshold in strain. In other words the defects become available only after a certain amount of deformation has occurred.

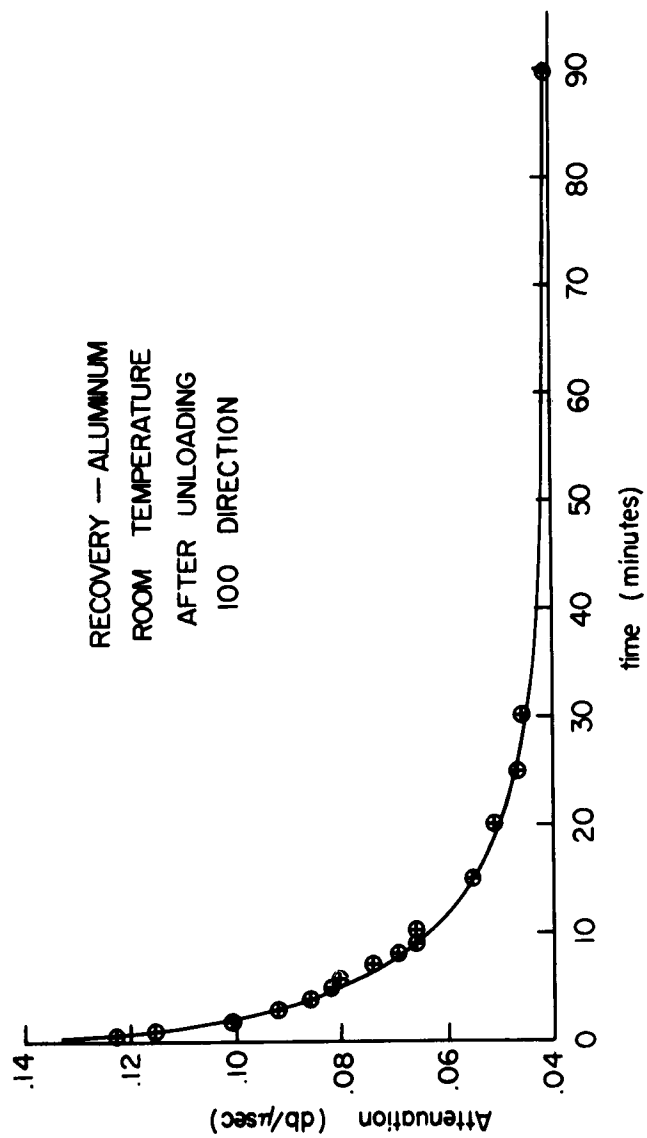


Figure 1
Recovery of attenuation as a function of time following loading and unloading.
Room Temperature. Deformation in $\langle 100 \rangle$ direction.

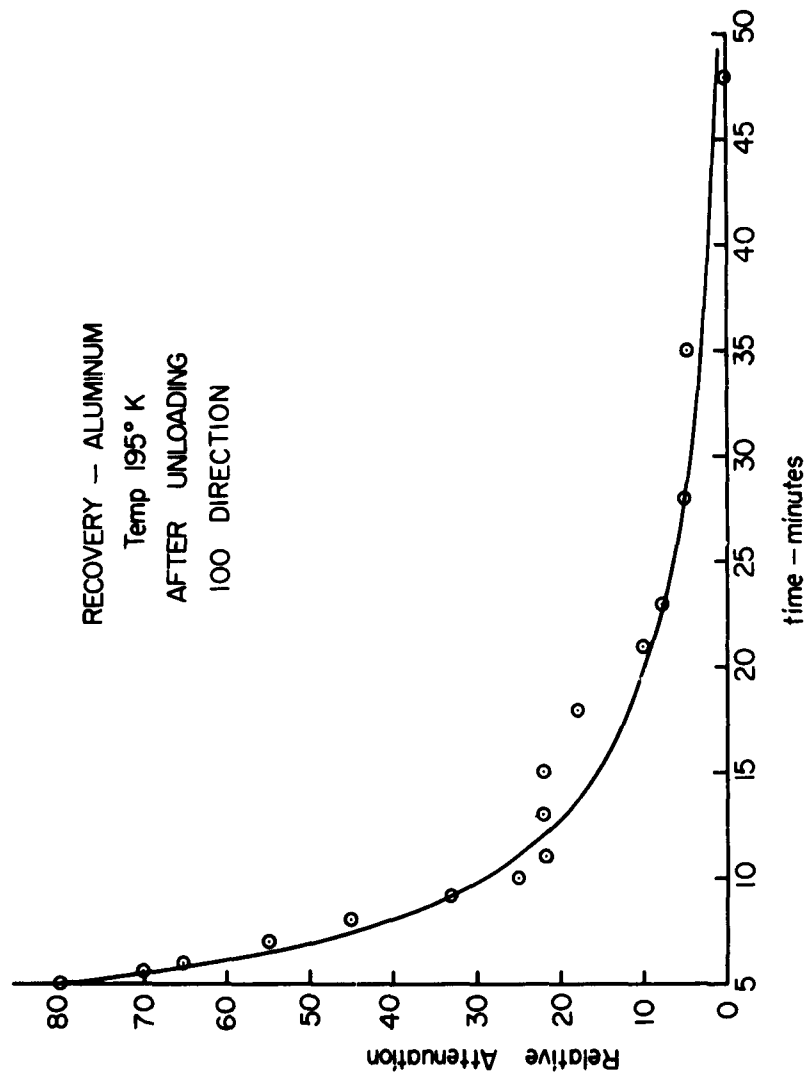


Figure 2

Recovery of attenuation as a function of time following loading and unloading. Temperature at 195°K during entire experiment. Deformation in $\langle 100 \rangle$ direction.

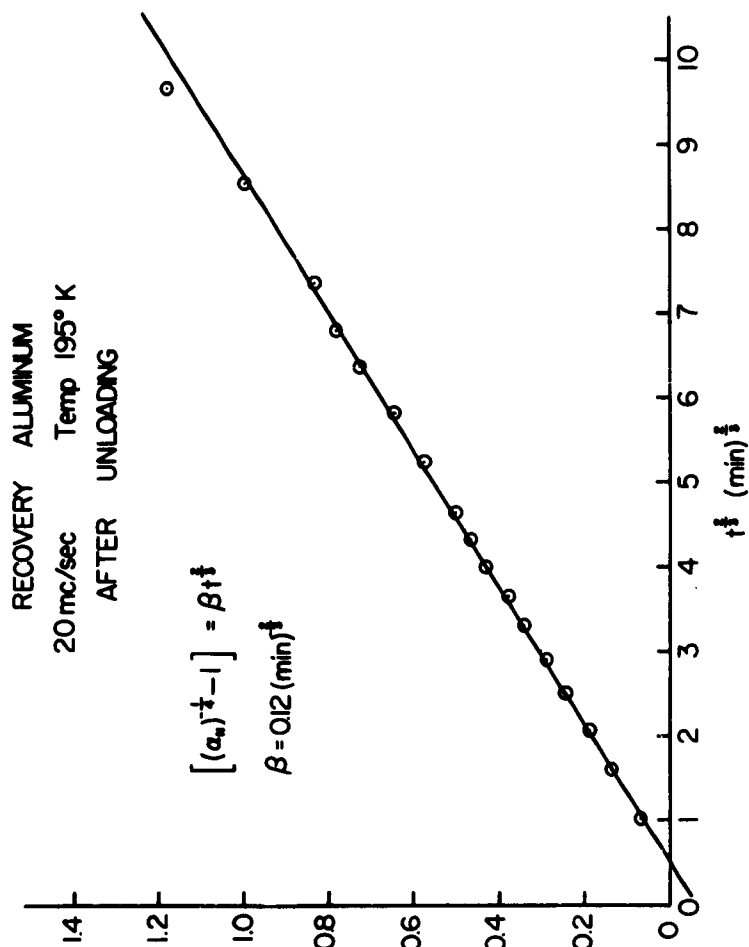


Figure 3
Values of $[(a_N)^{1/4} - 1]$ as a function of time $t^{2/3}$ during recovery.
Data taken at 195°K and after unloading.

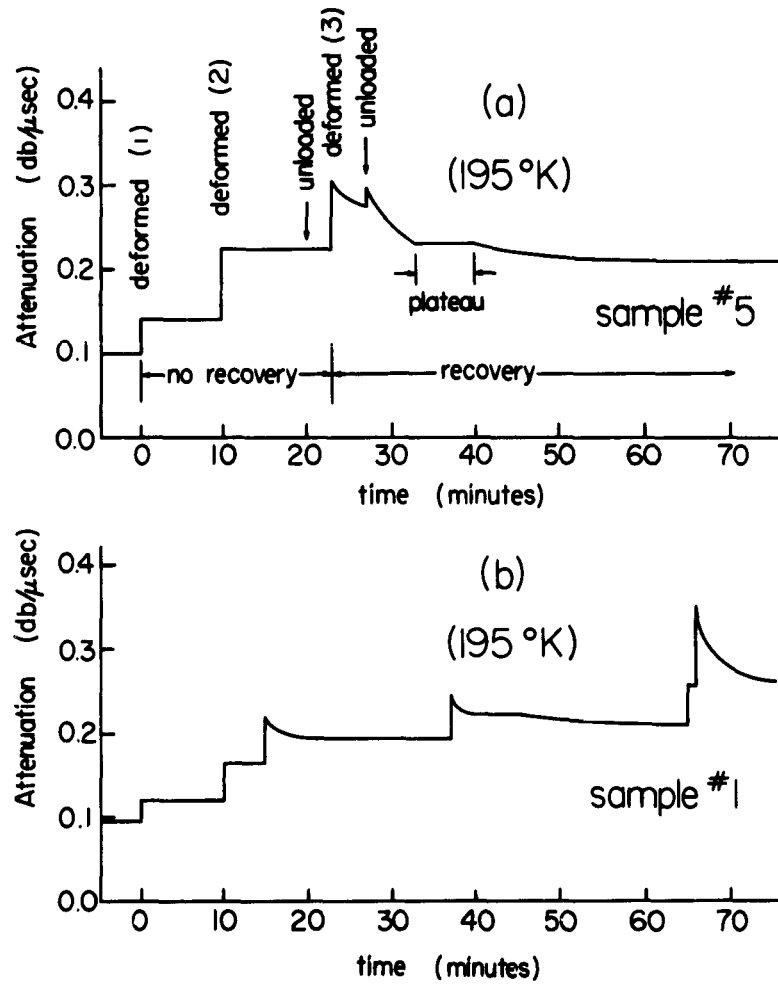


Figure 4

Attenuation as a function of time after loading of samples, (a) #5, (b) #1, at 195°K. Region of no recovery shown by flat steps following first (1) and second (2) deformations.

2. Anomalous Velocity Effect

Dislocation theory predicts an unusual behavior for ultrasonic velocity changes at high frequencies. Normally, the effect of pinning dislocations in crystals is an increase in velocity of ultrasonic waves (or elastic modulus) in the crystal. Pinning reduces the motion of the dislocations, and therefore the anelastic strain, so that only the purely elastic strain is measured in crystals with completely pinned down dislocations. However, it is possible, under conditions to be discussed here, for the velocity or modulus to decrease with pinning of dislocations. The latter effect will be termed anomalous. It is important both because an experimental check of this unusual prediction can be regarded as one of the strongest checks available to the theory, and because of the possible application of this effect to the study of deformation and irradiation processes.

The results of the relevant theory have already been used by Hikata, Chick, Elbaum and Truell⁽¹⁾ to account for the anomalous velocity change observed during deformation of aluminum single crystals. Since that time the physical nature of the cause of the effect has become clear, and a detailed and extensive examination has been made of the rather special conditions required to obtain the anomalous effect. At the same time a more complete mathematical description of the expected pinning behavior has been made including velocity calculations having quantitative validity at high frequencies. A comparison of this theory is made with the experimental results available to date.

The origin of the effect of dislocations on the elastic modulus and velocity may be understood with the help of Figure 1. In Figure 1A, the straight line segment along the x-axis between $x = 0$ and $x = l$ represents a dislocation loop of length l which is straight when no stress is applied. When a stress is applied, the dislocation loop bows out, but it is held back by the pinning points at the end, as in curve (1

of Figure 1A. If the stress is sinusoidal, with frequency ν , the displacement $y(x)$ is sinusoidal, with curve (1) representing the amplitude of the dislocation displacement. However, if the medium in which the dislocation segment vibrates is viscous, there will be a drag on the dislocation tending to oppose the motion. In real crystals, the viscosity is thought to be caused by the phonon gas through which the dislocation is being driven.

At low frequencies, the velocity of the dislocation is small, and the viscous drag may be neglected. In this case, the motion of the dislocation is limited only by the tension of the dislocation line, and a curve such as (1) of Figure 1A is obtained. At high frequencies, the velocity of points of the dislocation line remote from the pinning points is large, so that the viscous force is more important than the tension force. The amplitude of motion then becomes viscosity-limited, and is less than that obtained for low frequencies. Now, the dislocation segment oscillates over most of its length as a rigid rod, except at the end points, where the displacement is zero. The same transition in behavior from curve (1) to curve (2) occurs if the ultrasonic or driving frequency is held fixed and the loop length is increased, or if the frequency and loop length are held fixed and the viscosity is increased (for example, by increasing the temperature and therefore increasing the density of lattice vibration phonons).

Curve (2), however, represents the envelope of the amplitude of the motion. At any given instant therefore the shape of the dislocation displacement will not appear as in curve (2). The reason for this is that the phase of all points along the line is not the same. These points near the pinning points have a small maximum displacement and therefore a small velocity so that the viscous drag is small, and they are always in phase with the applied stress. On the other hand, points near the middle of the segment are approximately 90 degrees in phase behind the stress for

large viscous drags. As a result, the parts of the motion represented by curve (2) which are out of phase and in phase with the applied stress are as shown in Figure 1B. If the loop length ℓ is long, then the motion is out of phase (i.e., lags behind by nearly 90 degrees) over most of the loop length. The curve shown in Figure 1B also represents schematically the shape of the dislocation segment at two times differing by one quarter of the period of the motion.

In ultrasonic measurements, the out of phase and the in phase parts of the motion are measured separately. The out of phase motion leads to attenuation and the in phase motion leads to velocity changes of ultrasonic waves. The area under the curve of the in phase part of the motion is proportional to the anelastic strain contributed by the dislocation. The dislocation contribution to the strain is given by

$$\epsilon_{dis} = \frac{1}{\ell} \int_0^{\ell} b y'(x) dx$$

where $y'(x)$ is the real part of $y(x)$, b is the Burgers vector, and ϵ_{dis} can thus be thought of simply as the area under the real part of the dislocation displacement. The modulus change of the specimen is given by $\frac{M_0 - M(\omega)}{M_0} = \frac{\epsilon_{dis}}{\epsilon_{el}}$, where $M(\omega)$ is the modulus measured at frequency ω , and M_0 is the modulus measured at infinite frequency. ϵ_{dis} is the dislocation contribution to the total strain and ϵ_{el} is the elastic strain. Since the velocity of an ultrasonic wave is given by

$$V = \sqrt{\frac{M}{\rho}}, \quad \frac{\Delta V}{V_0} = \frac{V_0 - V(\omega)}{V_0} = \frac{1}{2} \frac{\Delta M}{M_0}$$

where ρ is the density of the solid. This then represents the velocity or modulus decrease of an ultrasonic wave in a crystal containing dislocations. As the frequency is increased, this area decreases and the ultrasonic velocity therefore increases, as the dislocation is no longer able to follow the rapidly varying external stress. Such a dispersion has been observed in NaCl between 10 and 100 megacycles/sec by Granato, deKlerk and Truell⁽³⁾.

Experimentally it is usually easier to vary the average loop length or resonant frequency ν_0 than it is to vary the measurement frequency ν , as for example in irradiation or in deformation and recovery experiments. If instead of varying the stress wave frequency with fixed loop length, one varies the loop length with fixed frequency, the anomalous velocity effect appears. Figure 1C shows how the displacements of Figure 1B change when a pinning point is added. At low frequencies, when a pinning point is added, the area of the in phase component of the displacement is decreased, and so the ultrasonic velocity increases, i.e., $\Delta v/v_0$ decreases and $v(\omega)$ increases. However, at high frequencies, addition of a pinning point forces the part of the dislocation near the newly added pinning point to be in phase with the applied stress so that the in phase component of displacement pops out, increasing the area, and decreasing the ultrasonic velocity. It is clear from Figure 1C that the effect is in general a small one, since at high frequencies, only a small part of the displacement is in phase with the external stress. If more pinning points are added, the in phase component eventually becomes pinned out completely. As this limit is approached the pinning points get close enough together to interact, giving the normal velocity effect because the more pinning point regions that are added the more tension limited segments are added until a limit is reached. Also, from Figure 1C, one sees that adding pinning points to very long dislocation loops has little effect on the attenuation when the motion over most of the length of the loop is viscous drag limited. Eventually, when the average loop length is made small enough, the attenuation decreases with pinning.

In this way it is seen that for long enough loop lengths (or large enough frequencies or large phonon densities or temperatures), velocity or modulus measurements are sensitive to conditions near the pinning points while attenuation (or decrement) measurements are sensitive to the viscous drag or specific damping caused by dislocation-phonon scattering. Under the specific conditions just mentioned, velocity

measurements are especially appropriate for investigating dislocation - pinning point interactions while attenuation measurements are more relevant for dislocation-phonon interactions.

A quantitative theory for the attenuation and velocity of ultrasonic waves in crystals containing dislocations has been given by Granato and Lucke⁽⁴⁾. The model is based upon the analogy between the motion of a dislocation loop and that of a vibrating string proposed by Koehler⁽⁵⁾. The results are given in the form of infinite series. The first term of the series gives a sufficiently accurate description of the attenuation. Because of the simplicity of this attenuation result, the effect of a distribution of loop lengths on the result is also not difficult to obtain. For velocity, the first term of the series is also sufficiently accurate for frequencies up to about that for which the inflection point appears in the dispersion curve. As mentioned at the end of second paragraph, page 8, for higher frequencies (where the velocity reduction $\Delta v/v_0$ is small) the first term of the series is not quantitatively adequate and a series expression must be used. However, calculations show that the first term of the series still gives all the qualitative results, including the anomalous velocity effect. The effect of a distribution of loop lengths has not been considered. Simple analytical results, giving explicitly the effects of the various variables, will be used for the present discussion.

For the purpose of studying the effects of pinning or unpinning of dislocations it is convenient to express the changes in attenuation and velocity in terms of loop length or resonant frequency ω_0 . We have chosen to use the variable $y \equiv \frac{\omega_0}{\omega}$ where ω_0 is the resonant frequency of the dislocation loops and ω is the frequency at which measurements are taken. As the loop length is decreased by pinning, y increases since the resonant frequency increases. Expressed in this way, the

attenuation becomes

$$\alpha(y) = K \frac{d}{\omega^2} \left\{ \frac{1}{(y^2 - 1)^2 + (d/\omega)^2} \right\}$$

and the velocity change is given by

$$\frac{\Delta v}{v_0} = \left(\frac{v_0 - v(\omega)}{v_0} \right) = H \frac{1}{\omega^2} \left\{ \frac{y^2 - 1}{(y^2 - 1)^2 + (d/\omega)^2} \right\}$$

$$d = B/A$$

where

$$K = \left[\Omega 8.68 \times 10^{-6} \left(\frac{4Gb^2}{\pi^2} \right) \frac{\Lambda}{A} \right]$$

$$H = \left[\Omega \left(\frac{4Gb^2}{\pi^2} \right) \frac{\Lambda}{A} \right]$$

G is the elastic shear modulus, Ω is the orientation factor, b is the Burgers vector, and Λ is the dislocation density. The factor 8.68×10^{-6} is needed to give the attenuation in the commonly used units of decibels per microsecond.

In the above, the parameter d is a measure of the damping. These curves for various frequencies of interest are plotted in Figure 2 for an assumed value of the damping constant d of $7.4 \times 10^9 \text{ sec}^{-1}$.

For a given measurement frequency, as the resonant frequency of the dislocation loops is increased by pinning, as for example with irradiation, from $y = 1$ the attenuation decreases from a maximum value, while the velocity at first decreases (anomalous effect), passes through a minimum and then increases (normal effect). The velocity curve has a minimum at $y_m^2 = 1 + d/\omega$, at which point the attenuation is half the maximum value. This is also the point at which the decrement is a maximum. One can locate on the velocity curves of Figure 2, values of y for an assumed initial resonant frequency. For example, if $\nu_0 = 300 \text{ mc/sec}$ is assumed the velocity curve for $\nu = 30 \text{ mc/sec}$ would have $y = 10$ as the value of y at the start of irradiation or deformation. By drawing a plot of the locus of all points for each assumed

resonant frequency, one finds a set of curves such as those shown in Figure 2 for 150, 200, and 300 mc/sec.

The intersections of the second set of curves, shown on the velocity diagram, with the curves just described, show the values of the velocity with respect to the elastic value v_0 at each ultrasonic frequency for a given resonant frequency of the dislocation loops. For example, if the resonant frequency of the dislocation loops is $\gamma_0 = 300$ mc/sec, then for all frequencies below about 20 mc/sec, the velocity is constant (i.e. independent of frequency), while for larger frequencies, the velocity is higher. This describes the normal dispersion effect.

If, however, measurements are made at constant frequency with varying loop length or varying ω_0 , the curves (see also Figure 3) show under what conditions the anomalous velocity effect occurs. For example, suppose the resonant frequency of the dislocation loops is 150 mc/sec to start with. If now the resonant frequency is increased to 300 mc/sec by some pinning mechanism, then the velocity increases at 10 mc/sec, giving the normal effect. At 20 mc/sec, the velocity at first starts out with zero slope and then increases. That is, there is initially no change in velocity in spite of the fact that the attenuation is decreasing rapidly as a function of ω_0 at this frequency. For higher frequencies, the velocity at first decreases with pinning before increasing. It is easy to see that the magnitude of the velocity reversal must be a small one. Suppose, for example, that the velocity change measured at low frequencies is 1% (this corresponds to a 2% change in modulus, and larger changes arising from dislocation damping changes are seldom seen at megacycle frequencies). Then from Figure 2, it is evident that the magnitude of the velocity reversal effect cannot be expected to be greater than about 0.1%. Figure 3 is an enlarged section of Figure 2, and it shows somewhat more clearly the size of effect, or change in velocity, that one can expect to the left of the velocity minima for different resonant frequencies and various

measurement frequencies. The exact size depends upon how far to the left of the minimum the intersection of curves in Figure 2 or Figure 3 occurs. The effect of the higher order terms in the series expression for the velocity, as well as the effect of a distribution of loop lengths, will be to broaden out slightly the minimum and to cause these curves to intersect the abscissa below $y = 1$. Figure 4 shows the comparison of velocity from the first term of the velocity expression from dislocation damping theory⁽⁴⁾⁽⁶⁾ and the velocity calculated from a series expression in which as many terms were used as needed to insure a small remainder. The dashed curves of Figure 4 (long and short dashes) are the values of $\frac{\Delta v}{v_0}$ calculated from the series expansion. This does not change anything qualitatively but has the effect of reducing somewhat the magnitude of the anomalous velocity effect to be expected.

From the above discussion, necessary conditions for observing the anomalous velocity effect can be established. One needs the resonant frequency to be low initially (i.e., large loop lengths) and velocity measurements sensitive to at least one part in 10^4 . It might be thought that specimens of sufficiently high purity would have long enough loop lengths. Attempts to find this effect in irradiated, undeformed, high purity aluminum and sodium chloride have been unsuccessful. However, the effect has been found in deformed crystals. Evidently, light deformation produces loop lengths of sufficient size. Deformation and irradiation (or recovery after deformation) can be expected to give similar but oppositely directed changes. Irradiation or recovery should produce pinning (i.e., increasing y). On the other hand, deformation should produce increased loop lengths for very small deformation (decreasing y), followed by decreasing size of average loop length after large deformation. Although irradiation or recovery experiments should be simpler physically because the dislocation density does not change at the same time that the average loop length does, it seems, at present, to be necessary to use deformation to produce suitable conditions. If aluminum single crystals can be made with higher purity and fewer and longer dislocations in such a way as to make the loops longer by a factor of five the effect should be observable using Co^{60} gamma irradiation.

In this section we discuss first the results observed during deformation, and then the simpler case of the changes which occur on recovery.

In Figure 5 results by Hikata, Chick, Elbaum and Truell⁽¹⁾, for the velocity, attenuation, and stress as a function of strain are shown for an aluminum single crystal. The direction of polarization of the ultrasonic shear was such that dislocations in the primary glide system were not seen by the ultrasonic wave. As a function of deformation the velocity at first increases a small amount (a few parts in 10^4) before decreasing. Figure 6 shows this velocity reversal effect for three principal directions in these specimens. Normally at low frequencies it would be expected that the velocity should decrease with deformation since the dislocations produce an anelastic strain. However, this behavior and magnitude of effect is just what should be expected if small deformation produces large dislocation loop lengths.

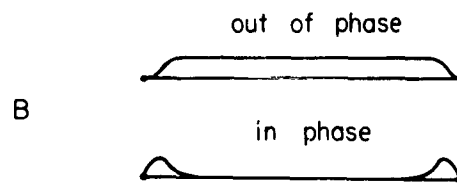
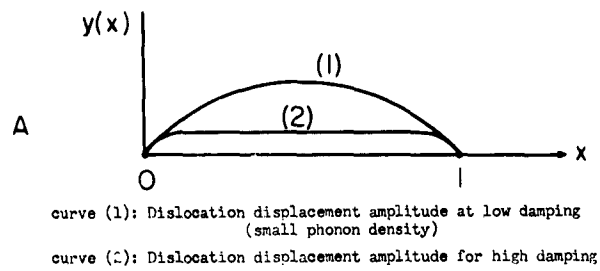
At high strains where the dislocation density becomes large, the normal reduction of velocity with deformation is found because the lengths are now much shorter. This small velocity reversal is usually found in high purity aluminum. It should be noted that $\Delta v/v_0 = \frac{(v_0 - v(\omega))}{v_0}$ does not change sign; the quantity $\frac{\Delta v}{v} = \frac{v_1 - v(\omega)}{v_1}$ plotted in Figure 5 refers not to v_0 , the purely elastic velocity, but to v_1 measured initially before deformation. The value of v_0 , the purely elastic velocity, for a perfect aluminum crystal is not known. Presumably the value of v_0 lies somewhere above any point of the curve. The observed effect is consistent with the expected anomalous effect. No other explanation of the observed behavior has been found.

It might be expected that, if the deformation were stopped in a strain interval where the velocity reversal was taking place, the pinning which would occur during recovery and as a function of recovery time should show the anomalous effect more

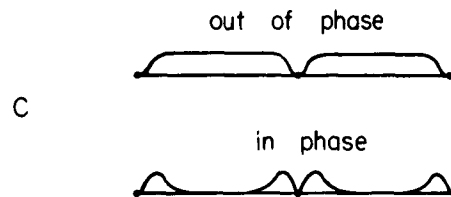
definitely. This is difficult to arrange at room temperature in aluminum because recovery occurs so quickly. Presumably, recovery occurs as a result of pinning of dislocations by the deformation induced point defects⁽⁷⁾. However, in NaCl, recovery is slower at room temperature, and an example of work in progress by Hikata, et. al. is shown in Figure 7.

Here the results of the recovery, under no load, of velocity and attenuation in NaCl after a small deformation are shown. As in the case of aluminum, there is a velocity reversal during deformation. This is not shown here. During recovery, the attenuation decreases from the very beginning, showing that pinning is occurring, but the velocity does not change for at least several minutes. After a time delay, the velocity increases in the normal way. The total velocity change is small (several parts in 10^4). This is the behavior expected if the starting point is near the minimum of the velocity curve in Figure 2 or Figure 3.

It is believed that the verification of these predictions of the theory constitutes one of the strongest tests available of the validity of the dislocation damping theory. It is expected that the effect can be used with profit in the study of deformation, recovery, and irradiation processes.



Out of phase and in phase component of dislocation displacement for high damping.



Change in Figure 1B when pinning point is added at center of dislocation loop.

Figure 1
Displacement of a dislocation under stress. schematic.

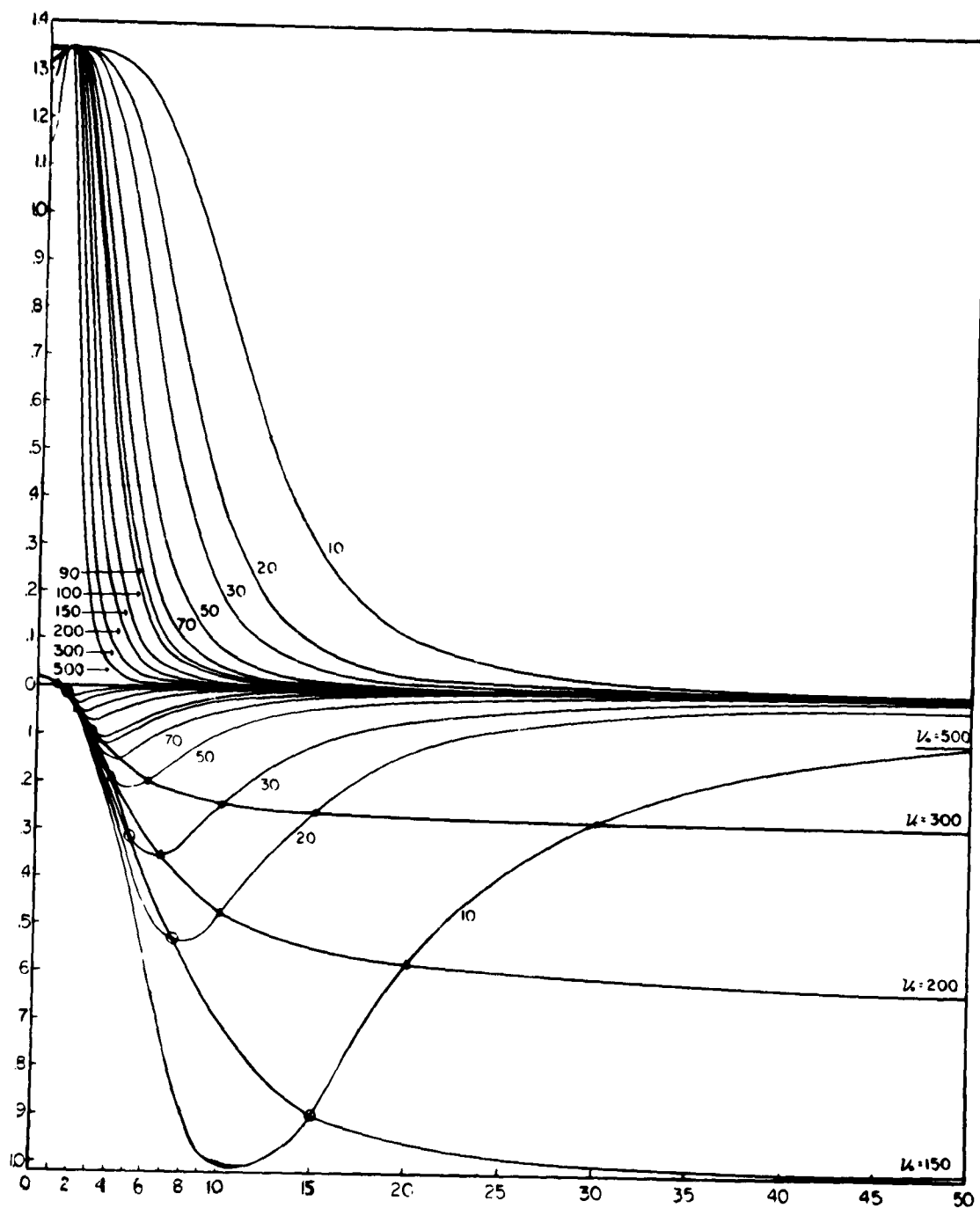


Figure 2

Normalized attenuation and velocity change for a solid containing dislocations as a function of (ω_0/ω) .

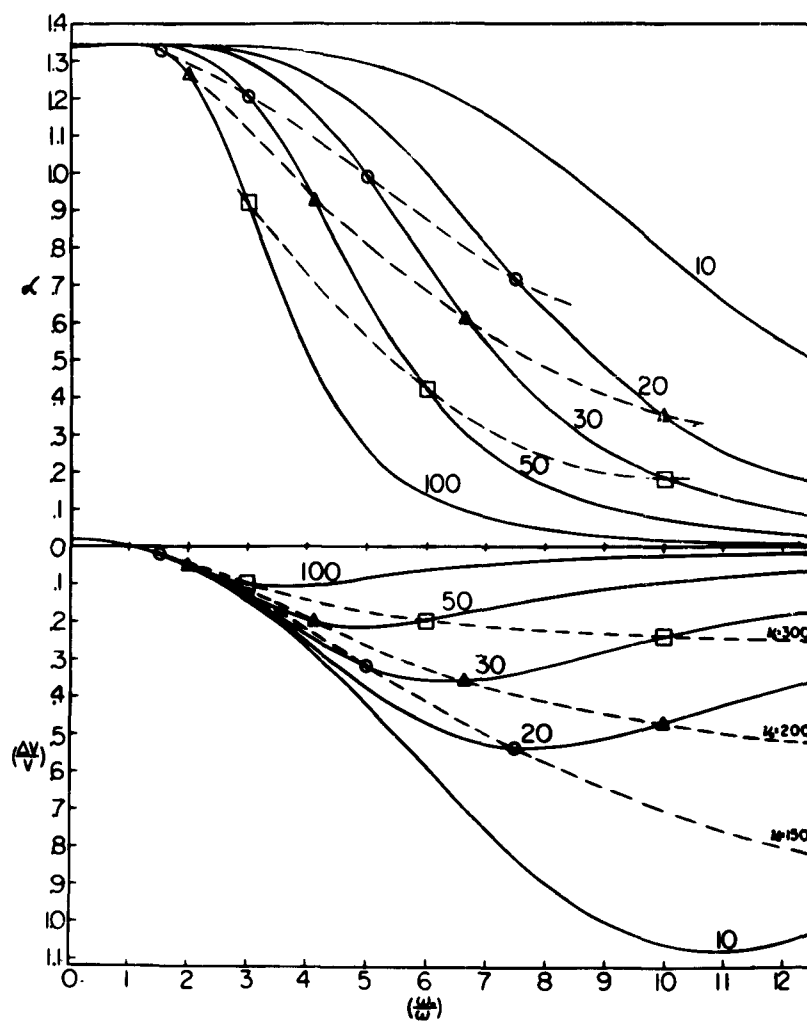


Figure 3

Enlarged section of Figure 2 showing α and $\frac{\Delta v}{v_0}$ and for low values of $(\frac{\omega}{\omega_0})$

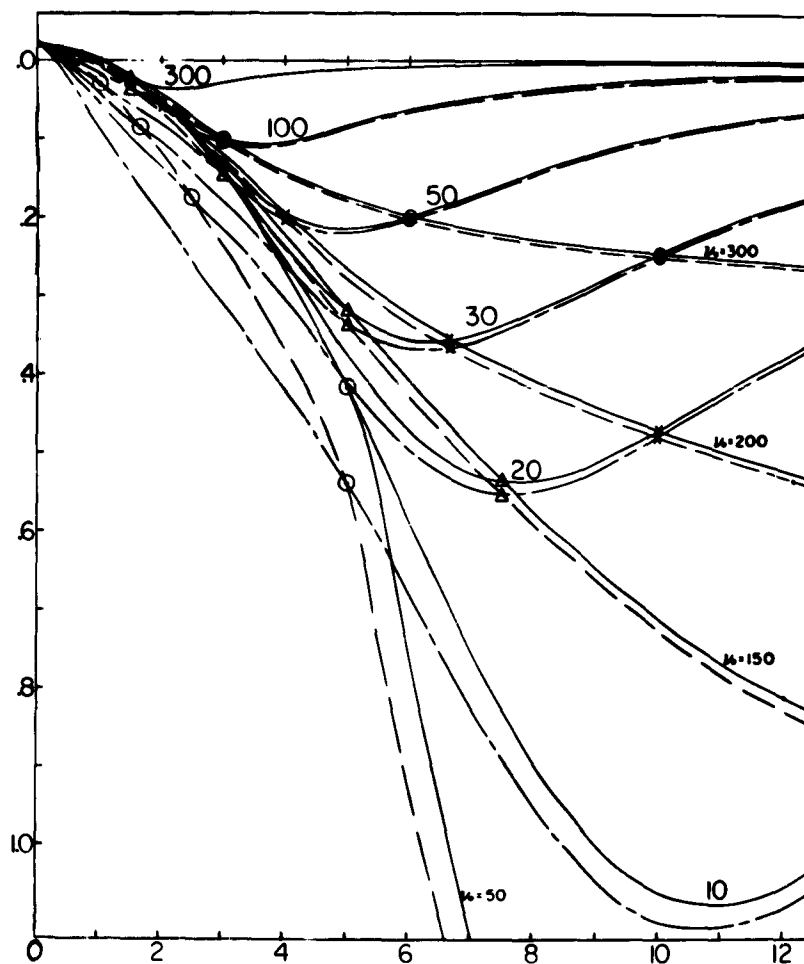


Figure 4
Comparison of $\frac{\Delta v}{v_0}$ curves calculated from first term of velocity expression
(solid line) with a number of terms of series expression for velocity (dashed line)

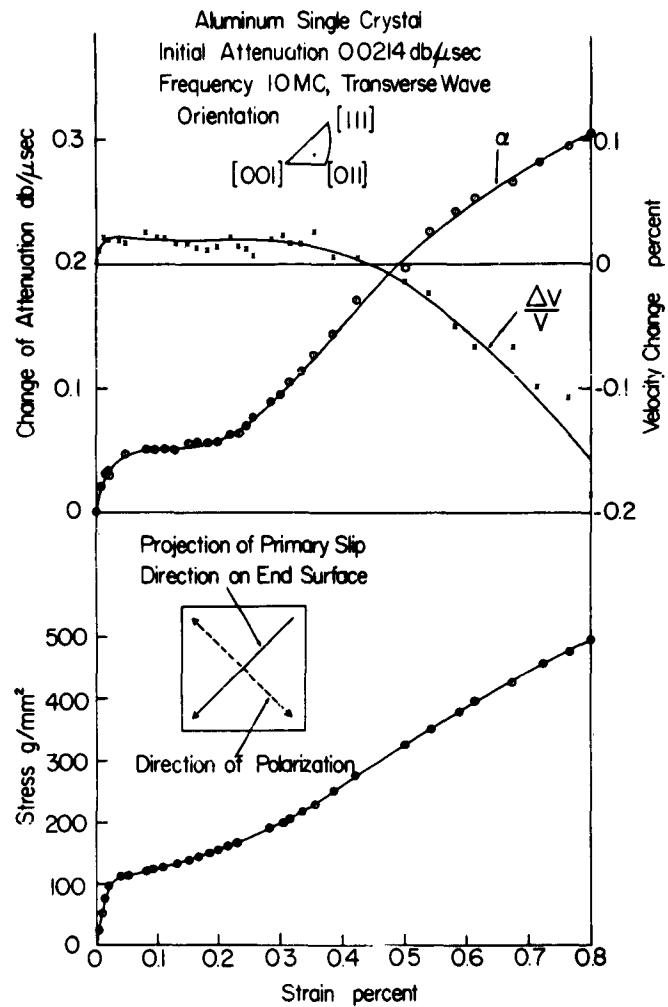


Figure 5

Stress, shear wave attenuation and velocity change as a function of total strain in aluminum. Hikata et al.

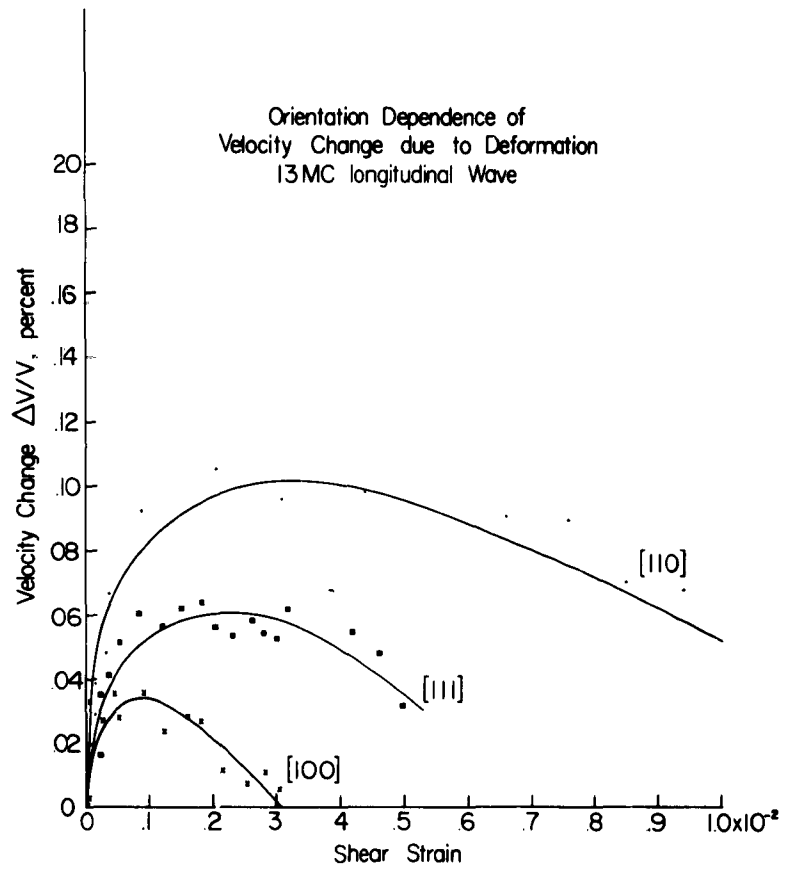


Figure 6

Longitudinal wave velocity change $\frac{\Delta v}{v}$ for $\langle 100 \rangle$, $\langle 111 \rangle$ and $\langle 110 \rangle$ orientation as a function of shear strain. Hikata et al.

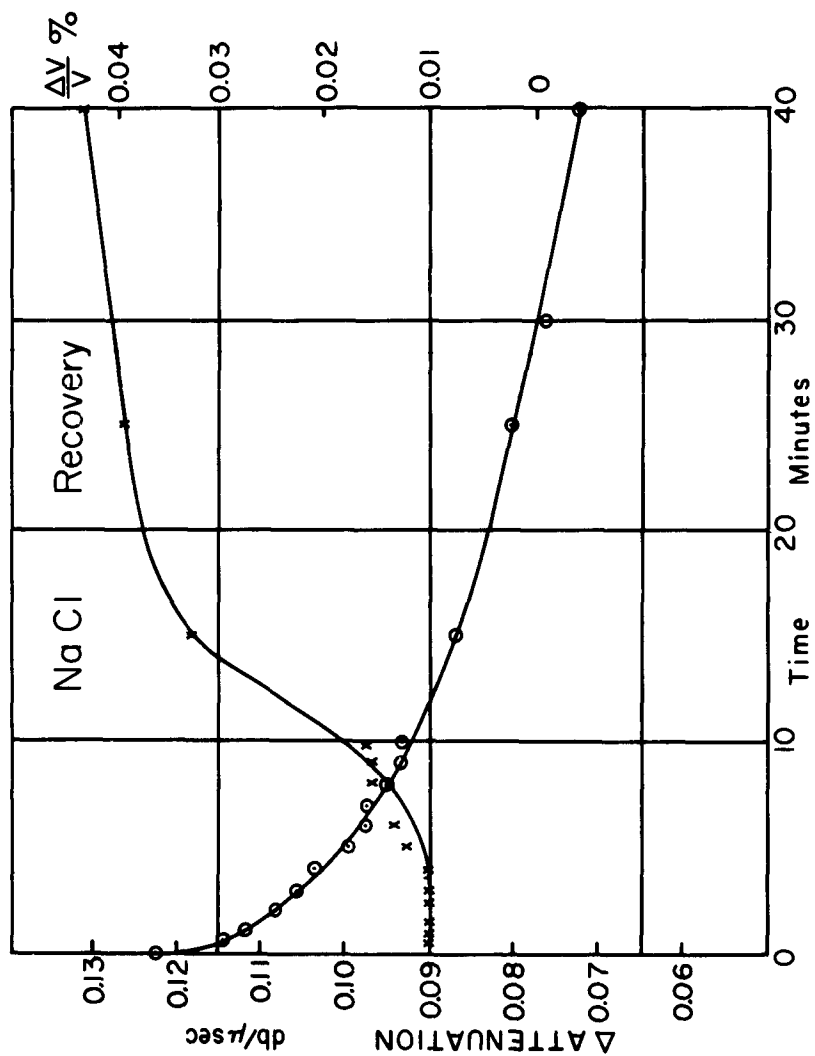


Figure 7
Recovery of attenuation and velocity in slightly deformed sodium chloride.
Compressional waves at 10 mc/sec in $\langle 100 \rangle$ direction.

3. Deformation in Ionic Crystals

This section on the deformation of ionic crystals includes discussion of certain results obtained from measurements of ultrasonic attenuation and velocity as well as electrical conductivity measurements and load-strain measurements. All of these measurements were made concurrently during deformation. Despite the fact that the ultrasonic measurements and the conductivity measurements compliment one another and provide more information than either would do by itself, we have chosen to present the results separately because the discussion seems clearer this way. As a consequence this section is divided into parts (a) and (b); part (a) is concerned mainly with dislocation damping in sodium chloride during plastic deformation and part (b) is concerned with an electrical charge study in sodium chloride during plastic deformation.

Part (a)

Sodium chloride single crystals have been deformed in tension, at room temperature. The specimens used have a rectangular cross-section 6mm x 25mm and were about 100mm long. The external surfaces were perpendicular to $\langle 100 \rangle$ type direction (they were bounded by $\{100\}$ type planes). The tensile stress was applied parallel to the long axis of the specimen, i.e., along a $\langle 100 \rangle$ type direction. For this direction of the tensile stress, four slip systems, each consisting of a $\{110\}$ plane and a $\langle 110 \rangle$ direction contained in that plane, are equally stressed in shear. For the geometry chosen here, plastic glide is expected to occur predominantly on two of the four equally stressed systems, as shown in Figure 1. This is so because for the two "expected" slip systems the slip path is considerably shorter (four times, in this case) than for the two "unexpected" slip systems.

When a longitudinal wave is propagating in the z direction of Figure 1 (direction of the applied tensile stress) it will have shear stress components in the same slip systems as the tensile stress. This wave will, therefore, interact with dis-

locations in these slip systems and the attenuation changes of the wave, upon plastic deformation, will reflect changes in the density and loop lengths of these dislocations. A longitudinal wave propagating along the y direction in Figure 1 will not have any shear components in the two "expected" slip systems, but will have such shear components in the other two (the "unexpected") of the four equally stressed slip systems. Changes in the attenuation of this wave will, thus, reflect changes in the density and loop length of the dislocations in the two "unexpected" slip systems, but not in the two "expected" ones.

Following this scheme, two longitudinal waves, with a frequency of 20Mc/sec, were propagated in the indicated directions and are labeled 1 and 2 respectively; the position of the quartz transducers are shown in Figure 1. The changes in the attenuation of these two waves were measured simultaneously by means of two separate ultrasonic attenuation units while the specimens were deformed in tension at a strain rate of 0.002 in./min. The relations between stress and strain and the corresponding changes of attenuation with strain, obtained during these experiments, are shown in Figure 1. Essentially identical results were obtained on four specimens. The attenuation of wave 1 increases monotonically with strain, as expected from the proposed model of deformation. The attenuation of wave 2 increases very slightly for small deformations, then decreases below the original value, reaches a minimum and starts increasing again slowly.

The interpretation of the behavior of wave 2 is based on the following reasoning. The criterion for predominant slip on the systems with the shorter slip path does not become meaningful until dislocation motion has occurred over distances comparable to the shorter slip path. Before this condition is fulfilled, slip may be expected to occur (in small amounts) on all four equally stressed slip systems. The small increase in attenuation of wave 2 is attributed to the initial increase

of the dislocation loop length in the "unexpected" slip systems, which is detected by this wave. For further deformation, after a small amount of strain hardening, dislocation motion stops in the "unexpected" slip systems, but the attenuation 2 starts to decrease. This decrease is attributed to a shortening of the average dislocation loop length in the two "unexpected" slip systems, due to many intersections by moving dislocations in the two "expected" systems, where plastic glide continues*.

The attenuation starts to increase again when the two "unexpected" slip systems begin to contribute to the plastic deformation. This view is supported by the fact that an increase in the rate of strain hardening (an inflection point in the stress-strain curve) coincides with the minimum in attenuation of wave 2. Ultrasonic velocity measurements of wave 1, carried out concurrently with attenuation measurement, showed a normal velocity decrease as a function of increasing strain at this stage of deformation.

The following conclusions, are readily drawn from the results of this study.

(1) Plastic glide in equally stressed slip systems of sodium chloride single crystals depends on the length of the slip path. (2) A method has been found for studying the effect of dislocation loop length on damping, for an approximately constant dislocation density. (3) The ultrasonic attenuation of a crystal (the part that depends on dislocation damping), along some crystal directions, can be decreased by small amounts of plastic strain, when the deformation geometry is properly selected.

* This is believed to be the only instance of dislocation damping measurements, made during deformation, under conditions such that the loop length is decreased, while the dislocation density remains essentially unchanged. In previous studies, shortening of loop length, without changes in dislocation density, was achieved by means of Cobalt 60 gamma ray irradiation.

The study of ultrasonic attenuation behavior discussed here is part of a larger investigation which includes the study of the electrical charge associated with dislocations in alkali halides.

Part (b)

Electrical charges developed during plastic deformation of alkali halides have been the subject of several recent studies.

The deformation-induced charge flow was first reported by Stepanow⁽⁸⁾ in 1933, who accidentally found, during his experiments on conductivity change of sodium chloride due to plastic deformation, a potential difference between the ends of the specimen in the absence of an applied field. The charge dissipated through the measuring circuit over the temperature range from 30°C to 170°C depended on the shape of the specimen. Although Stepanow could not explain this effect, he was able to make it negligibly small (by proper choice of experimental conditions) during his conductivity measurements.

In 1955, two reports concerning the charge effects appeared. Caffyn and Goodfellow⁽⁹⁾ investigated NaCl, KCl, NaI, KI, and KBr single crystals from various sources and found a potential difference between the electrodes on the surfaces of all the crystals upon the application of a compressional stress, though the amount of the potential differed from one crystal to another. The effect was temperature independent up to 180°C but then decreased with increasing temperature, being almost negligible at 250°C. They interpreted this charge effect as a result of local stress inhomogeneities at the surface without giving any specific mechanism.

Fischbach and Nowick⁽¹⁰⁾ studied NaCl single crystals under compressional stress. In this case, however, the deforming load was applied to a smaller area on one face of the specimen than on the other in order to produce purposely inhomogeneous deformation. Under this stress gradient, negative charge flowed in the external circuit away

from the side of the crystal to which the higher stress was applied. Even under applied electric fields as large as 10^3 v/cm, the direction of the initial charge flow produced by deformation was determined by the sense of the stress gradient rather than by the direction of the applied electric field. The current was transient and decayed with time in an approximately hyperbolic manner, and was observable for a time of the order of minutes when the stress increment which had produced it was left on. There was no appreciable current in the reverse direction even on removing the total load from the crystal. Successive cycles of removal and reapplication of load produced successively smaller effects. From this experimental evidence they concluded that the charge carriers must be charged dislocations.

Fischbach and Nowlok⁽¹¹⁾ (1958) extended the above work and included a study of the conductivity change due to deformation. They showed that the observed charge effects could not be explained by a contact potential difference, by thermal effects due to the deformation, or by diffusion in the stress gradient of free vacancies produced by the deformation. Their reasons for suggesting charged dislocations are as follows: Jogs on an edge dislocation line in NaCl may have an effective charge of $\pm e/2$, the sign depending on whether the jog occurs at a positive or negative ion as suggested by Seitz⁽¹²⁾. In the normal state of the crystal, a dislocation line is expected to have as many negative as positive jogs and therefore to be electrically neutral. However, when a dislocation line is in motion, vacancies may "evaporate" at a jog, thereby changing the sign of the charge at the jog. Thus when a negatively charged jog generates a positive-ion vacancy, it becomes a positively charged jog. A dislocation in motion may be expected to have equal numbers of negative and positive jogs only if cation and anion vacancies are formed with equal ease. The calculations of Mott and Littleton⁽¹³⁾ indicate, however, that the energy required to form a negative-ion vacancy is somewhat larger than that required to form a positive-ion vacancy.

Therefore, a moving edge dislocation line may be expected to acquire a net positive charge due to the preferential loss of positive-ion vacancies from jogs. These positively charged dislocations move into the crystal from the regions of stress concentration leaving behind a net excess of (negatively charged) cation vacancies". Although the above reasoning should be reexamined from the point of view discussed later, their effort in establishing the fact that the charge carriers in deformation-induced charge flow in NaCl are dislocations, should be strongly emphasized.

Based on the calculation by Mott and Littleton mentioned above, Frenkel⁽¹⁴⁾ (1948) and Lehovec⁽¹⁵⁾ (1953) independently arrived at the same conclusion that, when the temperature is raised from absolute zero an excess of positive-ion vacancies is emitted from the surface into the crystal, leaving a net positive charge on the surface. That is, in equilibrium the bulk of the crystal is electrically neutral, but there is a positive charge on the surface, balanced by an equal and opposite negative charge cloud penetrating some distance into the crystal. Eshelby et al⁽¹⁶⁾ (1958) made the important advance of suggesting that a similar space charge should occur around a dislocation, since jogs at dislocations can serve as sinks and sources for vacancies within the body of the crystal. They showed, furthermore, that in ionic crystals dislocations should generally be charged and be surrounded by a cylindrical Debye-Huckel cloud of the opposite sign. As a result of the above a substantial part of the critical shear stress of such crystals is attributable to the electrostatic attraction between a dislocation and the surrounding charge cloud. In the course of the analysis they introduced the concept of the "isoelectric point p". This point occurs at a temperature for which the concentration of positive-ion vacancies, that would obtain in the absence of impurities and without the requirement of electrical neutrality, becomes equal to the actual concentration of the positive-ion vacancies.

At the temperature of the isoelectric point dislocations are uncharged and the yield stress vanishes. (assuming that the yield strength of an ionic crystal is determined entirely by the electrostatic interaction between the charged dislocations and charge cloud surrounding them). The results they obtained in the experiments on temperature dependence of yield stress of NaCl crystals showed the isoelectric point to be at 320°K . This led to the conclusion that the free energy of formation of positive-ion vacancy in NaCl is less than 0.6 eV, unless the divalent impurity concentration is less than about 10^{-9} . Even if some of the impurity is precipitated such a value would seem unreasonably low, as they stated. According to this model, however, dislocations in equilibrium in an ionic crystal already possess an excess of charged jogs of one sign; it is not necessary for dislocations to be set in motion in order to acquire a net charge, contrary to the model proposed by Fischbach and Nowick mentioned above.

Amelinckx, Vennik and Remaut⁽¹⁷⁾ (1959) examined NaCl crystals under cyclic bending. They first bent a crystal statically introducing excess dislocations of one mechanical sign, and then brought the specimen into vibration in the frequency range of 10-1000/s. The charge observed on the electrodes placed on the concave as well as convex side was of the same sign for each half cycle (straightening or further bending) of the alternating stress. They made no statement about the sign of the charge on the dislocations.

In an extension of the above work, Remaut, Vennik and Amelinckx⁽¹⁸⁾ (1960) reported that the electrical signal decayed in amplitude during continued stressing. When the crystal was left at rest for some time, the signal returned approximately to its original value. The electrical signal was only observable if the amplitude of vibration exceeded a certain critical value. All these experimental facts were explained qualitatively by the model that positively charged dislocation oscillates

relative to the charged vacancy cloud surrounding them.

Sproull⁽¹⁹⁾ (1960) took a different approach to this problem. He applied instead of stress, a strong electric field to a bent crystal of LiF, and studied the motion of dislocations due to the field through the change of the bend. The experimental facts showed that the sign of the charge on the dislocations was positive. This means that, following Eshelby et al.⁽¹⁶⁾, the "isoelectric point" must have been below the experimental temperature (room temperature). Placing the isoelectric point at 0°C, and using the value of about 10^{-4} e.s.u./cm as the amount of charge on a dislocation, which was deduced from the experiments, Sproull estimated the energy of formation of positive-ion vacancy to be 0.3 eV. This value is again unreasonably low compared with what is accepted at present (about 0.6 eV).

Remaut and Vennik⁽²⁰⁾ (1961) studied NaCl crystals under cyclic bending, tension and compression on bent specimens and pulse stressing. For crystal tested under cyclic bending, a marked difference in amplitude dependence of electrical signals was found between an unannealed specimen and one annealed at 600°C for 48 hours after the static bending. The electrical effect was much smaller and showed little amplitude dependence in the bent and then annealed specimen. Tension and compression tests on bent specimens showed that the electrical signal coming from opposite faces (concave and convex faces) of the specimen were of opposite sign, contrary to what was observed during cyclic bending. However, no mention was made of the relationship between the sign of the signal, the face where the signal was developed, and the polarity of the stress (tension or compression). The shear stress at which the electrical signal started to increase rapidly was approximately 75g/mm^2 .

Vennik, Remaut, and Dekeyser⁽²¹⁾ (1961) extended this work. It was stated in this report, for the first time, that moving dislocations behave as if negatively charged. From the experimental facts that doping with Cd^{++} ions had no effect on the

sign of the signal and on its magnitude, although other tests, such as ionic conductivity, absorption spectra after irradiation, showed a marked influence of impurity, they concluded that the uptake of positive-ion vacancies by moving dislocations must not be considered as an explanation for the origin and sign of this effect. Instead, they suggested that the negative sign of the dislocations results from the boiling off of an excess negative-ion vacancies during the movement of the dislocations, without giving any theoretical basis. It is also reported that if the specimen was deformed by two different saw-tooth pulses of the same amplitude but of different duration, then signal corresponding to the pulse with longer duration was larger than the other.

Rueda and Dekeyser⁽²²⁾(1961),⁽²³⁾(1961),⁽²⁴⁾(1963) carried out a series of indentation tests on ionic crystals containing various concentrations of positive and negative divalent ions. They reproduced Fischbach and Nowick's^{(10),(11)} experimental arrangements and confirmed that the polarity of the electrical signal observed depended on the degree of the surface roughness at the bottom where the electrode was placed. Doping the crystal with CdCl_2 up to 0.2% did not affect the sign and the magnitude of the charge. Doping with Na_2O_2 of 0.2% reduced the magnitude of the signal considerably and addition of 1.0% Na_2O_2 reversed the sign completely. The measurements made by placing the electrode on various portions, relative to the indenter, of both top and bottom surfaces of the specimen showed some uncertainty between the results as far as the sign of the charge is concerned. Nevertheless they concluded that dislocations acquire negative charge during their motion by preferential uptake of vacancies of one sign, again without presenting any theoretical basis.

Caffyn and Goodfellow⁽²⁵⁾(1962) carried out four-point bending tests of NaCl . In this case, however, the specimen was cleaved in half and glued together again with

an Araldite cement containing powdered silver which served as an electrode lying on the elastic neutral axis. Potential difference was measured between the electrodes placed on the surface of the composite specimen and the one lying on the neutral axis. The results were that both the concave and convex faces of the specimen were always positive with respect to the electrode at the neutral axis. In order to explain this effect they proposed the following model for the arrangement of dislocations in a bent specimen: "Since the stress in bending is largest at the surface and is zero at the neutral axis, dislocations of one mechanical sign move outwards and escape at the surface, while dislocations of the other mechanical sign move inwards and are stopped before reaching the neutral axis, provided the stresses just exceed the yield stress. These considerations apply both to the concave and convex sides of the specimen. Therefore the number of dislocations that move away from the neutral axis and escape to the surfaces is larger than the number that move towards the neutral axis. If dislocations carry a net charge of one sign, then the charge must be transferred toward the surface." From these considerations they concluded that the sign of the charge carried by dislocations is positive. The model concerning the dislocation distribution in a bent crystal was confirmed independently by observations of birefringence.

Caffyn and Goodfellow⁽²⁶⁾ (1962) extended the work further, using compression tests, to determine the effect of specimen size and shape, effect of rate of loading and the charge-strain relationship. Although they could not determine the sign of the charge on the dislocations by this method, they established that the stress at which the electrical signal begins to increase rapidly, corresponds closely to the macroscopic yield stress of the specimen. It is also reported that the magnitude of the potential effect was directly proportional to the rate of the loading, contrary to the Vennik, Remaut, and Dekeyser's⁽²¹⁾ results.

Caffyn and Goodfellow⁽²⁷⁾(1962) made a comment on the sign of the charged dislocations in NaCl. Although these authors obtained the same polarity of the electrical signal as that of Rueda and Dekeyser's⁽²²⁾ indentation tests (opposite to the results observed by Fischbach and Nowick⁽¹⁰⁾⁽¹¹⁾), they tried to explain the results from the point of view that dislocations carry a net positive, instead of negative charge. The argument simply depends on the matter whether dislocations come towards the indenter or move away from the indenter. So far, this problem does not seem to have been explained in a satisfactory manner.

Bassani and Thomson⁽²⁸⁾(1956) examined the association of positive-ion vacancies and various types of impurities withunjogged edge dislocations in NaCl. According to their calculation the vacancy has an association energy of 0.4 ± 0.2 eV, but impurities, both monovalent and divalent, have smaller association energies. This consideration led to the conclusion that the positive-ion vacancies will be pinned to the core of the unjogged edge dislocations and produce an excess negative charge there. In fact, their calculation indicates that vacancies of both signs have approximately the same association energy with dislocations. An excess of positive ion vacancies on the dislocations would have to come from the larger concentration of these vacancies in the crystal. However, in the presence of positive divalent impurities, these vacancies will combine with the impurities to form a neutral complex. Thus, one is led to expect a positive charge on the dislocations. In any case, once the dislocations break through the vacancy cloud surrounding them, upon the application of stress, these dislocations no longer have a net charge. Moreover, since the present study is concerned with the charge brought by dislocations to the surface, the configuration discussed by Bassani and Thomson is not likely to apply in this case. The argument by Remaut⁽²⁹⁾(1962), based on the work of Bassani and Thomson, on negatively charged dislocations can be disregarded.

Koehler, Langreth and von Turkovich⁽³⁰⁾ (1962) have recently extended the theoretical work of Eshelby et al.⁽¹⁶⁾ by solving the non-linear equation which gives the potential distribution in an ionic crystal and by proposing boundary conditions appropriate at a dislocation core. The results of this work indicate that the dislocation charge is positive at elevated temperatures and becomes negative at low temperatures. The temperature at which the change of sign occurs decreases with decreasing concentration of positive divalent impurities. In these calculations, however, no account is taken of positive ion vacancy and impurity associations, and of possible impurity precipitation. The numerical value of the charge calculated for the room temperature and for an impurity concentration of 10^{-5} , is unreasonably high; this point is acknowledged by Koehler et al. It is obvious from the above considerations, that the problem is far from being settled and that further work on this subject is needed.

The above discussion indicates clearly that serious uncertainties, both in experiment and theory, still exist on the subject of dislocation charge in alkali halides. The only unambiguous conclusion to date seems to be that an electrical charge does indeed develop during plastic deformation and that this charge is associated with moving dislocations.

The present study was undertaken in an attempt to clarify some aspects of this problem. In particular, it should be pointed out that screw dislocations are not expected to be charged, because of the geometrical configuration. One of the immediate purposes of this investigation was to verify this assumption experimentally.

"Optical quality" sodium chloride single crystals, supplied by the Harshaw Chemical Company, have been used throughout this study. These crystals were not doped intentionally; their impurity content is not known to us. The specimens have been deformed in tension parallel to their long axis at room temperature, with a strain

rate of 0.05mm/min, using an Instron tensile testing machine. The external surfaces of the crystal were perpendicular to $\langle 100 \rangle$ type directions (they were bounded by $\{100\}$ type planes). The experimental arrangement is shown in Figure 2. This specimen geometry was selected for the following reasons. When a tensile stress is applied to a sodium chloride crystal along a $\langle 100 \rangle$ direction, four slip systems, each consisting of a $\{110\}$ type plane and a $\langle 110 \rangle$ type direction contained in that plane, become equally stressed in shear. For the geometry chosen here, plastic shear strain is expected to occur predominantly on two of the four equally stressed systems, as shown in Figure 3. This is so because for these two systems the slip path is considerably shorter (four times, in this case) than for the other two. Two independent checks have confirmed the corrections of this assumption, as discussed later on.

Electrical potentials with respect to ground were used as a measure of the amount of charge developed during deformation. Two arrangements for the measurement of charge are used depending on the purpose of a particular experiment. In one series of experiments the charge is measured simultaneously on one wide and one narrow face. In another series of experiments the charge is measured on the two wide faces. Two electrodes are produced by spreading a thin layer of conducting silver paint over an area of about 3mm x 10mm in the locations shown in Figure 2. These electrodes are connected to two electrometers (Kiethley type 610A)* by means of two 6 feet long coaxial cables having a capacity of approximately 30 μ F/ft. In all cases the integrated charge is determined as a function of strain.

Ultrasonic attenuation measurements have been carried out during deformation (concurrently with charge measurements) in order to verify the validity of the assumption concerning the "expected" and "unexpected" slip systems. The details of this

* The input impedance of the electrometers is 10^{14} ohms.

part of the study were reported elsewhere⁽³¹⁾. It is sufficient to mention here that the correctness of the above hypothesis was confirmed by this method. The specimens were also viewed in polarized light, during deformation, in order to verify whether slip detectable by this method appeared on the "unexpected" slip system. A low power microscope with a linear magnification of 20 was used for this purpose. Here again the results were consistent with our hypothesis.

Figure 4 shows the stress-strain, and charge-strain relationship found in the first series of experiments. The charge developed on the wide face increases rapidly with deformation in the beginning and then goes through a maximum. A much smaller amount of charge, which rapidly approaches a limiting value, also appears on the narrow face of the specimen. Several experiments performed in this manner have given results in agreement with the above, in so far that the absolute value of the charges developed on the narrow faces of the specimen were much smaller than those on the wide face of the specimen*. However, the sign of the charge measured was positive in some cases and negative in other cases and no systematic behavior was observed.

This ambiguity was resolved by the second series of experiments. In these experiments the charge was measured on the two sides of the crystal independently but simultaneously. The results of one of these experiments was shown in Figure 5. In this case charges of opposite sign are found on opposite faces of the same specimen. Strain measurements on both sides of the specimen revealed that the crystal was slightly bent before the experiment, and the negative charge appeared on the concave side of the bent specimen. Another experiment performed in the same manner gave

* In one case severe kinking of the specimen was observed and a reversal of charge was recorded; these results were discarded.

essentially the same results (the negative charge was again observed on the concave side).

In view of this observation, several experiments have been performed in which the specimens had been intentionally bent around the Y axis (see Figure 3) to a radius of about 1 meter. A four point bending jig was used for this purpose. After the intentional bending, one of the side faces of the specimen (concave or convex side) is scraped with emery paper over the area to be covered by the electrode (about 0.5 cm^2) thus introducing additional surface sources of dislocations. Electrodes are painted over the scraped area as well as on the opposite side of the specimen. After these treatments, the specimens were subjected to a tensile stress. Figure 6 shows the results of an experiment using a specimen which had the scraped area on the concave face. As soon as appreciable plastic flow started, both the concave and the convex sides developed positive charge. As plastic deformation continued the charge on the concave side changed sign, and eventually reached a large negative value, comparable with the charge observed on the concave side of accidentally bent specimens. On the other hand, the specimen having the convex side scraped did not show the reversal of the sign of the charge, as shown in Figure 7.

In the experiments performed so far, shorting out of the accumulated charge on one electrode did not affect the charge accumulated on the other electrodes. At room temperature the accumulated charge did not show any measurable recovery over a period of hours.

It is also found that the negative charge is always larger, in absolute value, by a factor of 1.5 to 2. The total integrated charge corresponds to a measured voltage of 10 to 30 volts or 2×10^{10} to 6×10^{10} electronic charges/ cm^2 (either positive or negative, depending on the side).

Three definite charge characteristics have been observed in this study:

- 1) The charge developed on the narrow face of a specimen is always much smaller than that on the wide face of the specimen.
- 2) When a slightly bent specimen is stressed in tension, negative charge appears on the concave side of the specimen and positive charge appears on the convex side of the specimen.
- 3) The negative charge observed on the concave side of a bent specimen is always larger, in absolute value, than the positive charge on the convex side of the specimen in the early stages of deformation (up to about 0.5% strain).

These charge characteristics during deformation of sodium chloride may be explained in the following way.

The dislocation geometry in the "expected" slip systems implies that when these two systems operate, edge dislocations move toward or away from the wide faces and screw dislocations move toward or away from the narrow faces of the specimen, as shown in Figure 8. Under these conditions, and in view of the fact that the screw dislocations are not expected to be charged, charge due to moving dislocations should appear on the wide faces only. However, when the tensile stress is first applied, some dislocation motion is expected to take place in all four equally stressed slip systems. This is so because the criterion for predominant slip on the systems with the shorter slip path does not become meaningful until dislocation motion has occurred over distances comparable to the shorter slip path. Before this condition is fulfilled, slip may be expected to occur (in small amounts) on all four equally stressed slip systems. Hence, at the very early stages of deformation some charge may appear on the narrow sides of the specimen. As deformation proceeds, slip occurs predominantly on the "expected" slip systems and not on the "unexpected" ones, because of the difference in the slip path, as discussed in the previous section. Thus in later

stages of deformation, the amount of charge should be much smaller on the narrow faces than on the wide faces. This is exactly what is observed in the first series of experiments in this study and provides an explanation of observation 1) above.

In order to explain the observations 2) and 3), it is necessary to assume that edge dislocations carry positive charge. Based on this assumption, the following model is proposed. During bending (accidental or otherwise) the dislocations of one mechanical sign, labeled A in Figure 9, migrate toward the neutral axis of the specimen cross-section. The dislocations of opposite mechanical sign, labeled B in Figure 9, move toward the external surfaces and may escape from the specimen. In this case, however, some piling-up of dislocations beneath the surface is expected, because the escape of dislocations is equivalent to the formation of a step on the surface (the "slip step"). Hence, work in addition to that required for moving dislocations must be done in order to supply the extra surface energy of the step, compared with the smooth surface. Thus in a bent specimen, the dislocation distribution is expected to be such that there is an excess of "type A" dislocations near the neutral axis and excess "type B" dislocations near the external surfaces. Caffyn and Goodfellow (13)(25) have proposed a similar model for a bent crystal.

The device used in the deformation experiments is such that when a tensile force is applied to a bent specimen, in a direction parallel to the chord, a bending moment tending to straighten out the specimen and an overall tensile stress will result. A tensile component must, therefore, be added to the tension on the concave side and to the compression on the convex side of the specimen, which is undergoing straightening due to the bending moment. The result is that both the convex face and concave face will be subjected to a net tensile stress (of different magnitude), as shown in Figure 9. Under the influence of a tensile stress, the dislocations labeled B (originally piled up beneath the surface) will move away from the concave face toward

the center. The negatively charged atmospheres of these dislocations are left near the surface, resulting in a negative charge on the concave side. The dislocations of type B, piled-up beneath the convex face, move out and give a positive charge on that side. The dislocations of type A, (originally piled-up near the center) move away from the convex face toward the center when a tensile stress is applied to the specimen. In this case a negative charge should result on the convex side and a positive charge on the concave side. It should be noted, however, that from the model proposed here the number of type A dislocations moving away from the convex side is smaller than the number of type B dislocations moving toward this side. A net positive charge should, therefore, appear on the convex side in the early stages of deformation. Similarly, the number of type B dislocations moving away from the concave side is expected to be larger than the number of type A dislocations moving toward it and a net negative charge should appear on the concave side.

Furthermore, as mentioned above, the net tensile stress is larger on the concave side and the number of dislocations moving away from this side is expected to be larger than the number leaving the crystal out of the convex side. This results in a larger negative charge, in absolute value, than the positive charge.

Thus the model proposed here together with the assumption that the edge dislocations carry positive charge are consistent with the observed results 2) and 3) mentioned above. Attempts to explain the results on the assumption that the dislocations are negatively charged were not successful.

The charge developed in the early stages of deformation is not thought to be associated with point defects carried to the surface because of the systematically observed positive and negative charge on opposite faces of the specimen. There is no reason to assume that charge point defects of a particular sign will migrate to or will be carried systematically to the same side of a bent crystal.

The results on the scraped specimens may be explained in the following way. When the surface is scraped, dislocation sources are introduced. It is assumed that, for any particular size of loop, equal numbers of dislocations of each mechanical sign will be introduced. Hence, upon the application of an external stress (the tensile stress in these experiments) equal numbers of loops of a particular size will tend to move toward the surface (out of the crystal) and away from the surface (into the crystal). However, the work required to move a loop of given size into the crystal is larger than that required to move a loop to the surface, because in the first case the total length of dislocation increases, whereas in the second case the loop is made to shrink. Moreover, the step on the surface (the slip step) associated with the dislocation loop decreases on moving the dislocation to the surface and increases on moving the dislocation into the crystal. Thus, additional work is required to expand the loop moving into the crystal.

It is assumed, therefore, that loops of a particular size and of the mechanical sign corresponding to the dislocation moving toward the surface will be activated, on the average, (or at lower stress levels) before those moving into the crystal. These loops will contribute a positive charge regardless of the charge developed due to the dislocation present in the crystal before bending. On the concave side a positive charge is thus observed at the start of plastic strain. This charge is subsequently reversed due to the piled-up dislocations and to the dislocations from surface sources which move into the crystal, while the surface sources that contribute dislocations moving toward the surface are being exhausted. On the convex side of the specimen, the dislocations from the surface sources merely add to the positive charge in the first stages of deformation.

The experimental result yet to be discussed is the maximum and the saturation (in absolute value) observed in the later stages of the charge-strain relationship.

(For example, the case such as Figure 4 for maximum and the case such as Figure 6 for saturation). Since the measurement refers to the accumulated charge on the electrodes, a decrease in absolute value can be accomplished either by carrying the charge away from the electrodes or by cancelling it with a charge of opposite sign. Strain measurements on both sides of the specimen revealed that at the stage of deformation where the maximum appears, the process of straightening out the originally bent specimen is completed. This means that there is no longer a distinction between the concave and convex sides. Therefore, at this stage, dislocations may move from the originally convex side, to the center, leaving a negative charge, while dislocations of the same mechanical sign move toward the originally concave side, bringing positive charge to that side. Under these circumstances the maximum in the charge-strain relationship should be observed. It should be pointed out here that the dislocations responsible for this process are not expected to be the ones newly created during the deformation for the following two reasons. Firstly, negatively charged atmospheres are not likely to form around these dislocations, in the course of the experiment, because diffusion of vacancies of a particular sign is involved, whereas at room temperature sufficient diffusion is not likely to occur. Secondly, the saturation of charge beyond a certain value of strain, observed in several cases, strongly suggests that intersections during the deformation do not produce a net excess of charged jogs of a particular sign. The formation of atmospheres around freshly created dislocations as well as the net excess of charged jogs of a particular sign on the "new" dislocations will be a function of strain rate and temperature. This aspect of the problem has not been explored in this study.

It is found that a charge is observed only on the crystals where edge components of dislocation loops emerge during plastic deformation. In the tensile experiments of a bent specimen (accidentally or intentionally) negative charge appears on the

concave side and positive charge appears on the convex side, and the negative charge is larger, in absolute value, than the positive charge, in the early stages of deformation. A direct determination of the sign of the electrical charge carried by edge dislocations was not accomplished in this study. However, the assumption that edge dislocations in sodium chloride carry electrical charge of positive sign and the model for the distribution of dislocations in bent crystals are consistent with results obtained in this study.

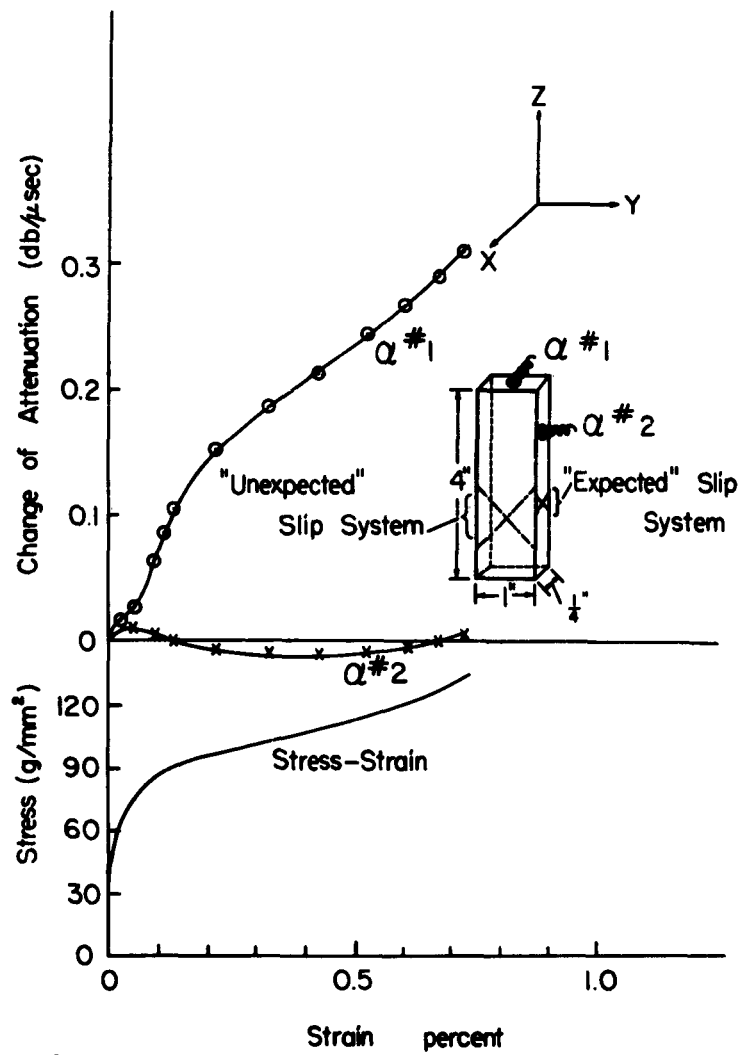


Figure 1
Comparison of attenuation changes at 20 mc/sec for compressional wave propagated in Z and Y directions together with the stress-strain relationship of the specimen.

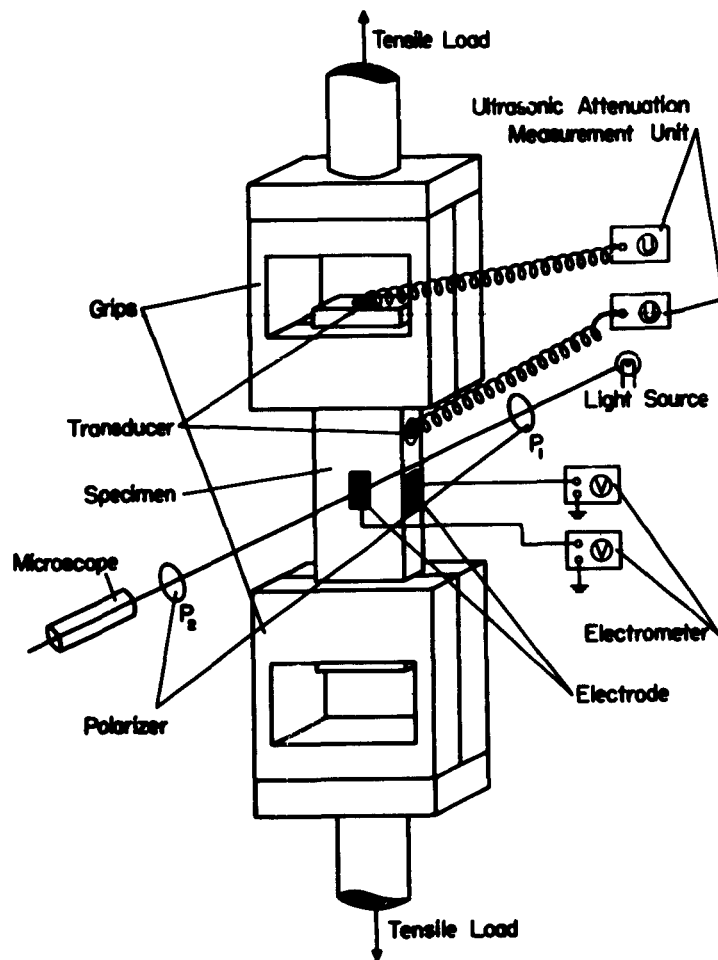


Figure 2
Schematic diagram of the experimental arrangement for the deformation of alkali halide single crystals.

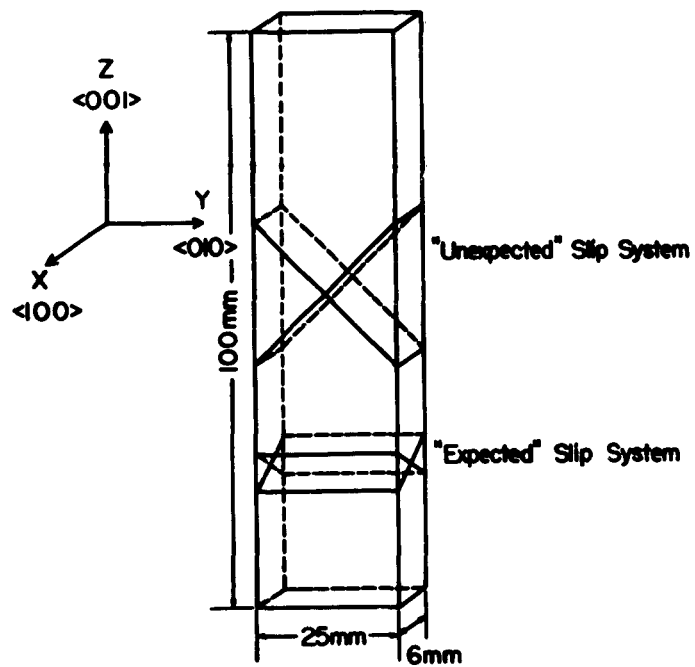


Figure 3
Dimensions and orientation of specimens; "expected" and "unexpected" slip systems are indicated.

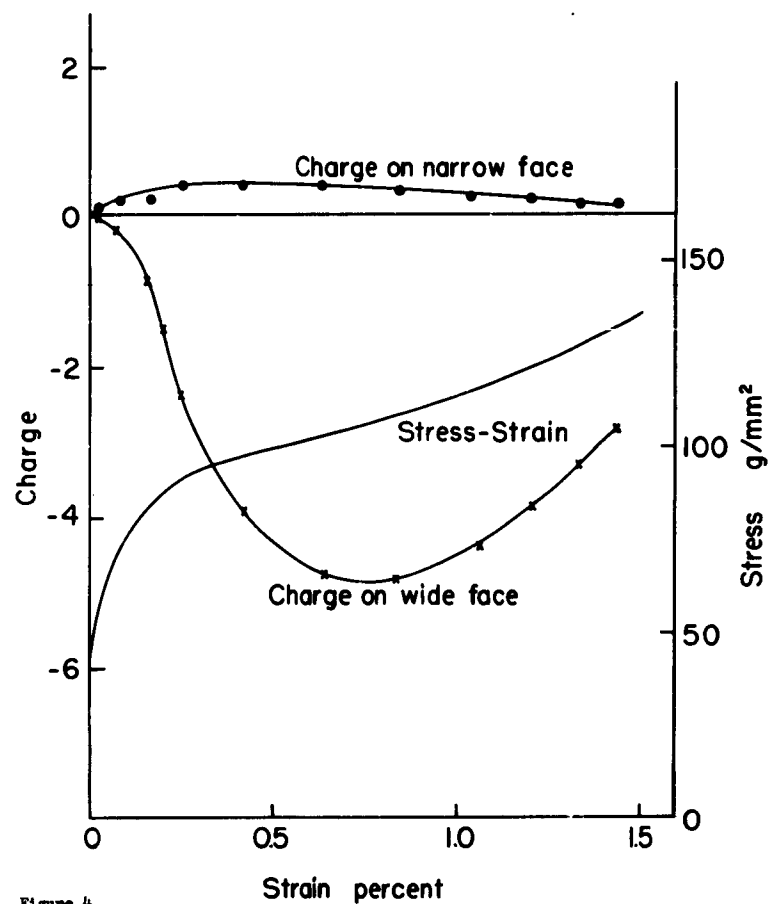


Figure 4
Comparison of the charge (in arbitrary units) developed on the wide face with the charge on narrow face, together with the stress-strain relationship for the specimen of sodium chloride.

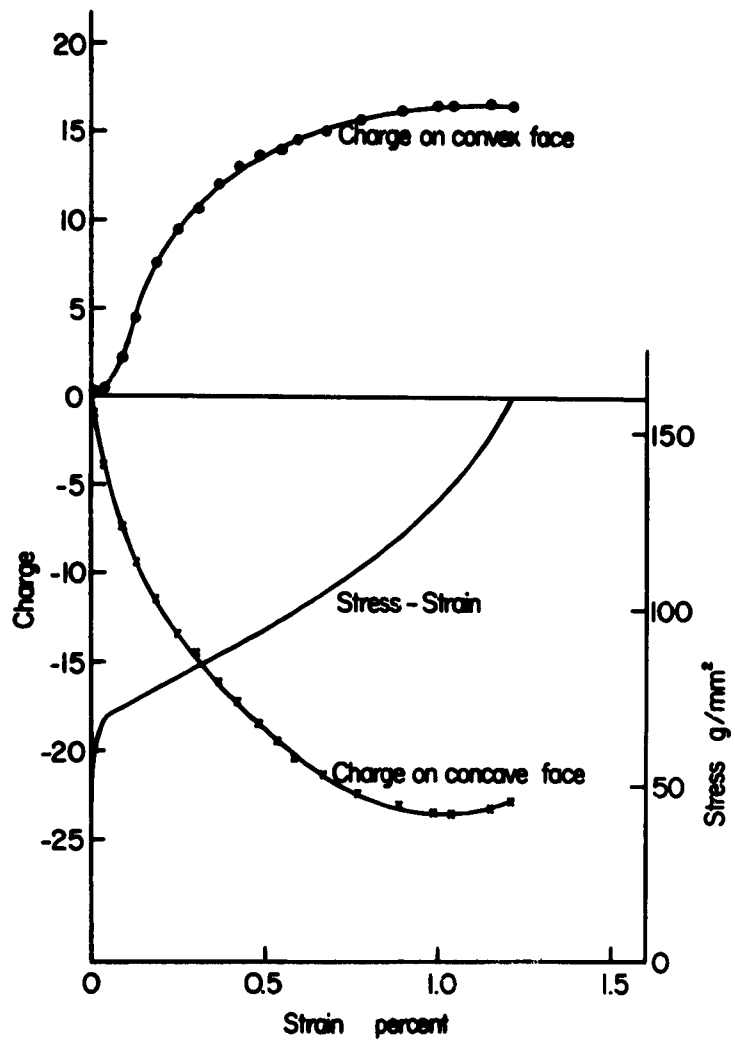


Figure 5

Charge-strain and stress-strain relationship of a bent sodium chloride specimen
(charge in arbitrary units)

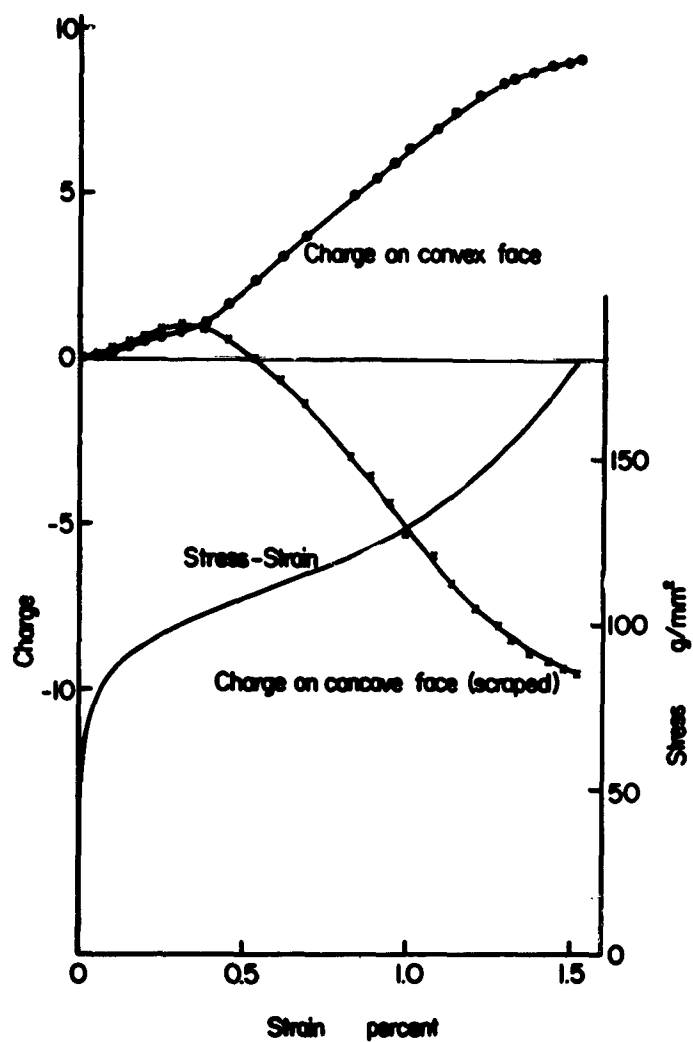


Figure 6

Charge-strain and stress strain relationship of a bent sodium chloride specimen. The electrode on the concave face was placed over an area scraped with emery paper. (charge in arbitrary units)

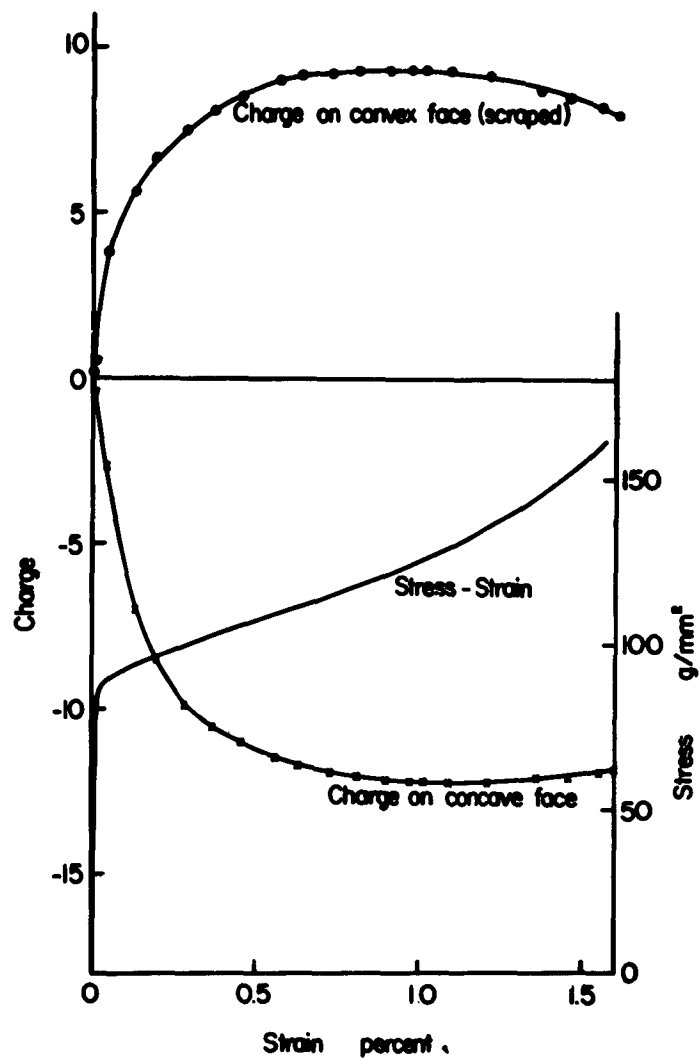


Figure 7

Charge-strain and stress-strain relationship of a bent sodium chloride specimen. The electrode on the convex face was placed over an area scraped with emery paper. (charge in arbitrary units)

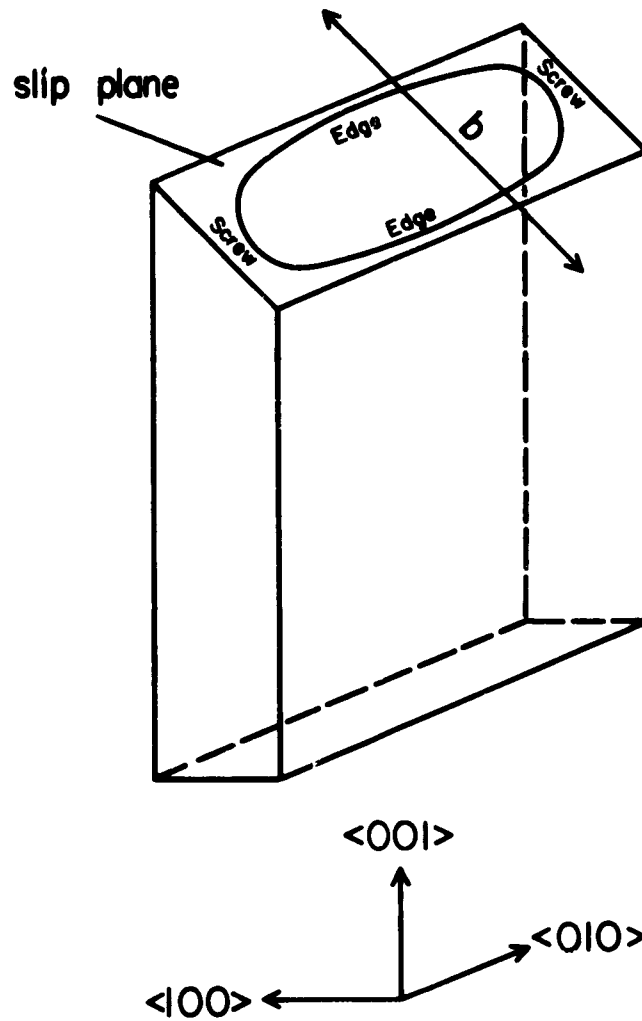


Figure 8

Dislocation loop on an "expected" slip plane, schematic.
 b : direction of Burgers' vector.

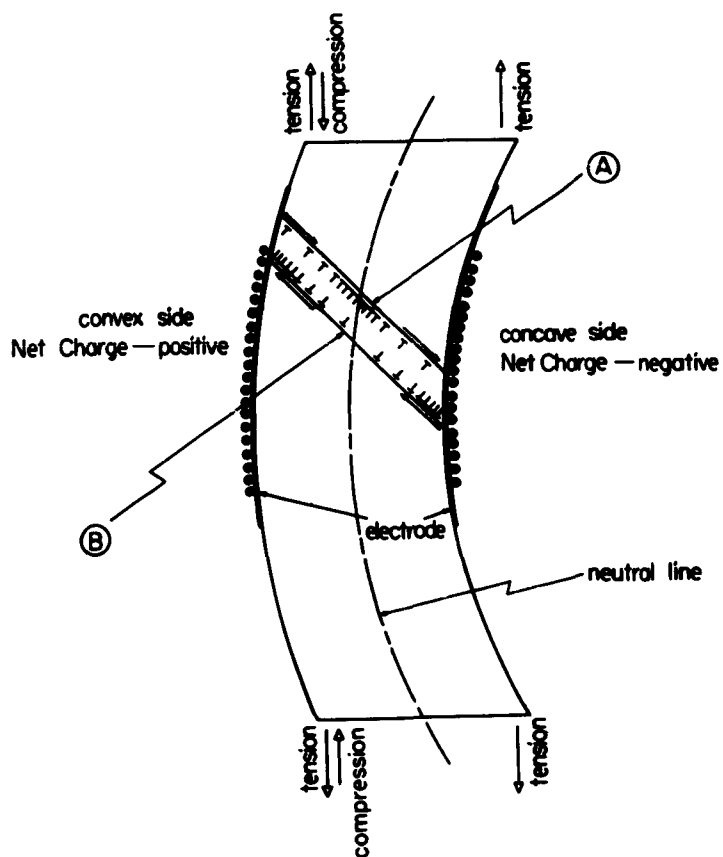


Figure 9

Dislocation distribution in a bent sodium chloride specimen, schematic.

4. Stress Cycling of Single Crystal Aluminum

Stress cycling of an aluminum single crystal has been carried out in several tests. The cycling has been done in tension and compression and the attenuation as a function of time has been recorded by means of the automatic recording attenuation measurement unit. The testing machine employed a mechanical drive giving a constant amplitude of displacement. The first cycling tests were of value mainly for checking techniques. The ability of the epoxy resin (glue) joints to stand the desired loads under cycling conditions has been determined and cycling tests have been run for periods of two to three million cycles. The cycling speeds have been both slow, six cycles per minute, and fast 1730 cycles per minute.

A number of interesting features have evolved from these exploratory experiments with stress cycling of single crystals.

The attenuation as a function of the number of cycles of stress exhibits a form that has been present in all of our previous results for polycrystalline aluminum as well. In particular the attenuation decreases at first and reaches a minimum and then increases as a function of number of cycles, and the minimum appears at about 1000 to 1500 cycles as shown in Figure 1. The cycling was done at the rate of 6 cycles per minute initially. At the 6 cycle per minute rate the attenuation can be followed completely by the automatic recording attenuation measurement unit and the pairs of triangles in Figure 1 show the maximum and minimum values of attenuation observed during a given cycle. The increase in attenuation following the minimum in the curve is clear up to the point in Figure 1 marked "Rapid Cycling Started" at which point the program of cycling was changed. Instead of continuing at the rate of 6 cycles per minute the cycling was carried out at 1730 cycles per minute and the points x in Figure 1 show only average values of attenuation because with rapid cycling the automatic recording unit does not follow in detail; it simply records an average value. At each value x ,

however, a pair of triangles appears also; this means that the rapid cycling was stopped and the slow cycling was carried on for a period, sufficient to obtain the data.

The start of rapid cycling obviously affected the trend that was being followed with slow cycling alone. Beyond the point where rapid cycling was started it appears that the attenuation increase was stopped and perhaps reversed as a consequence of the rapid cycling. The minimum in the attenuation curve suggests that (as with the polycrystalline samples discussed in previous reports) the decrease in attenuation may be associated with a decrease in the dislocation damping because of increased pinning which may arise both from increased dislocation density and an increased density of point defects produced during cycling. The decrease in dislocation damping loss as a function of cycling is eventually (around 1500 cycles) offset by an attenuation increase which may be a scattering effect arising from strain regions which could appear as a consequence of cyclic slip and the pile up of dislocations against barriers to form regions of gradients in the elastic constants, hence scattering regions. It is clear that the accumulation of such scattering regions (if this is the explanation) is much slower with single crystals than with polycrystalline and less pure aluminum because the attenuation increases with cycling much more rapidly in the latter case.

It may be noted that this idea concerning scattering regions and the difference between polycrystalline samples and single crystals can perhaps be tested to some extent by comparing an attenuation plot of the type of Figure 1 for cycling in a $\langle 111 \rangle$ direction, with the same experiment in the $\langle 100 \rangle$ direction. The slip behavior for cycling in the $\langle 111 \rangle$ direction should approximate that for a polycrystal much more closely than in a $\langle 100 \rangle$ direction. In other words the attenuation might be expected to increase more rapidly in the region beyond the minimum for cycling in a $\langle 111 \rangle$ direction.

Another feature of the dislocation damping changes that was examined in course of the stress cycling was attenuation recovery. At various points the cycling was stopped, and the attenuation decrease was observed as a function of time for periods of some hours. The attenuation recovery (for periods of five minutes and ten minutes) is shown in Figure 2 from 10^3 cycles to about 3×10^6 cycles. The amount of recovery decreases appreciably but rather slowly with cycling as compared with previous experiments involving polycrystalline samples of low purity in which the recovery disappeared more rapidly, and, in at least one case, disappeared altogether after 10^6 cycles. It is seen from Figure 2 that the rapid cycling does not appear to change the amount of recovery very much although the attenuation values (Figure 1) were raised appreciably when rapid cycling was started. The decrease in the amount of recovery as a function of cycling fits with the explanation given above in that during the cycling the dislocations become pinned down to a greater extent and the dislocation damping effects decrease. The subsequent increase in attenuation, if caused by scattering, would not influence recovery directly, although any new defects produced and capable of pinning would affect the rate and perhaps the amount of recovery.

Velocity measurements were not made in the course of the cycling. The automatic recording velocity measurement unit is not yet ready for such use. Velocity measurements would, if available, help to establish the nature of the attenuation losses.

It should be recorded that during the cycling discussed here the load in tension and in compression was 520 pounds per sq. inch for about 2×10^6 cycles at which point the load was increased in about 17 steps from 520 psi to 2620 psi finally. This final value of the load was roughly one and one half to two times the load that is usually needed to break such a specimen in a static tension test.

In addition to ultrasonic attenuation measurements, records were made of the stress vs. strain relation during cycling at slow speed (6 cycles per min.). Strains were measured by means of two SR-4 foil strain gages of one inch gage length cemented to opposite faces of the specimen. Loads were determined from strain gages attached to a ring dynamometer. The output of the strain and load gages was used to drive an x-y recorder. Results of these measurements are shown in Figure 3 for the first few load cycles, and for representative cycles at later stages in the test.

It was observed that the size of the hysteresis loop decreased at first with cycling at constant amplitude and constant speed. The behavior is more easily observed in Figure 4 where the width of the hysteresis loop (taken at zero load) is shown as a function of number of cycles. For constant stress amplitude the width of a loop is approximately proportional to the energy dissipated per cycle.

A comparison between the ultrasonic attenuation of Figure 1 and the plot of hysteresis loop width as a function of the number of cycles in Figure 4 shows some similarity. It is possible to argue that both types of measurement may be related to one another through a dislocation damping mechanism. The two sets of curves show a minimum and while not exactly at the same places they are roughly similar. At the start of rapid cycling the attenuation (Figure 1) increased abruptly, but the hysteresis loop width remained unchanged. As the rapid cycling proceeded (beyond 10^5 cycles the loop width decreased to a value smaller than at the previous minimum (between 10^2 and 10^3 cycles).

Beyond about 2×10^6 cycles the load was increased so that the stress increased from 520 p.s.i. to about 760 p.s.i. and the test continued at the higher cycling rate. The attenuation increased sharply as indicated by the final set of points in Figure 1. The hysteresis loop width also increased substantially as shown in Figure 3 and 4.

After about 5×10^5 additional cycles the width of the hysteresis loop had decreased.

The load was increased in a series of seventeen steps to the final load corresponding to a stress of roughly 2600 p.s.i.. During the tests at higher stresses the hysteresis loop became very much larger as shown in Figure 3. Attenuation measurements for the cycling at the higher stress values are not shown.

It seems clear that increasing the load in successive steps during cycling permits applying a much higher stress than would be possible either in static tension tests or in cycling tests at constant stress.

Attenuation measurements made before this cycling test and 36 days after the test show a final attenuation value slightly higher than the initial value (short lines at left and right in Figure 1) but much lower than the values attained during cycling. In other words the single crystal still has a large amount of recovery after 3×10^6 cycles at the various levels and with rapid and slow cycling.

Finally in connection with the stress cycling certain observations will be made regarding the automatic attenuation unit and its use in observing the attenuation during cycling in tension and compression. The attached chart in Figure 5 shows sections of the strip chart recording taken from the automatic recording attenuation measurement unit. This test was run mainly to check the techniques. At various stages the load was increased. Initially the load was 25 to 30 pounds in tension and an equal amount in compression. The load did not remain balanced in equal tension and compression for the run of about 10,000 cycles, and the load was increased a number of times during the run in order to find out what load the epoxy resin (glued) joints would stand during cycling. The cycling was done at six cycles per minute. The ultrasonic frequency was 10 mc/sec and compressional waves were used.

The changes in dislocation damping during the cycling are large and easily seen from comparison of the maximum-minimum attenuation values (for example a change of 0.14 db per microsecond in first cycle) with later maximum-minimum values (as for example a change of only 0.02 db per microsecond after only 60-70 cycles).

It should be noted that the first quarter of the first cycle (chart) is in tension between points marked (1) and (2) - i.e., sample is being loaded in tension. Between points (2) and (3) the sample is still in tension but is being unloaded, and it is at or near zero load at point (3). At point (3) the attenuation has not returned to point (1) because there has not been time for recovery to occur back to the attenuation value at (1). The load is changing most rapidly at point (3) and from (3) to (4) the sample is again being loaded but this time in compression. At point (4) the load is changing relatively slowly from (maximum load in compression) to unloading. The sample is again unloaded at point (5), and the whole cycle starts again. At each odd numbered point the load is reversing direction in going from unloading to loading in either tension or compression. At each even numbered point the change is from loading, in either tension or compression, to unloading.

In the early stages of cycling in this test the cycles are clear and easy to interpret; this is not the case in the later cycles because the loading in tension and compression is no longer equal because of the shortcomings and inadequacies of cycling equipment. It is clear from this and from much longer test described above that for a given load the attenuation or dislocation damping dies out with continued cycling just as in our early tests with relatively impure polycrystalline aluminum.

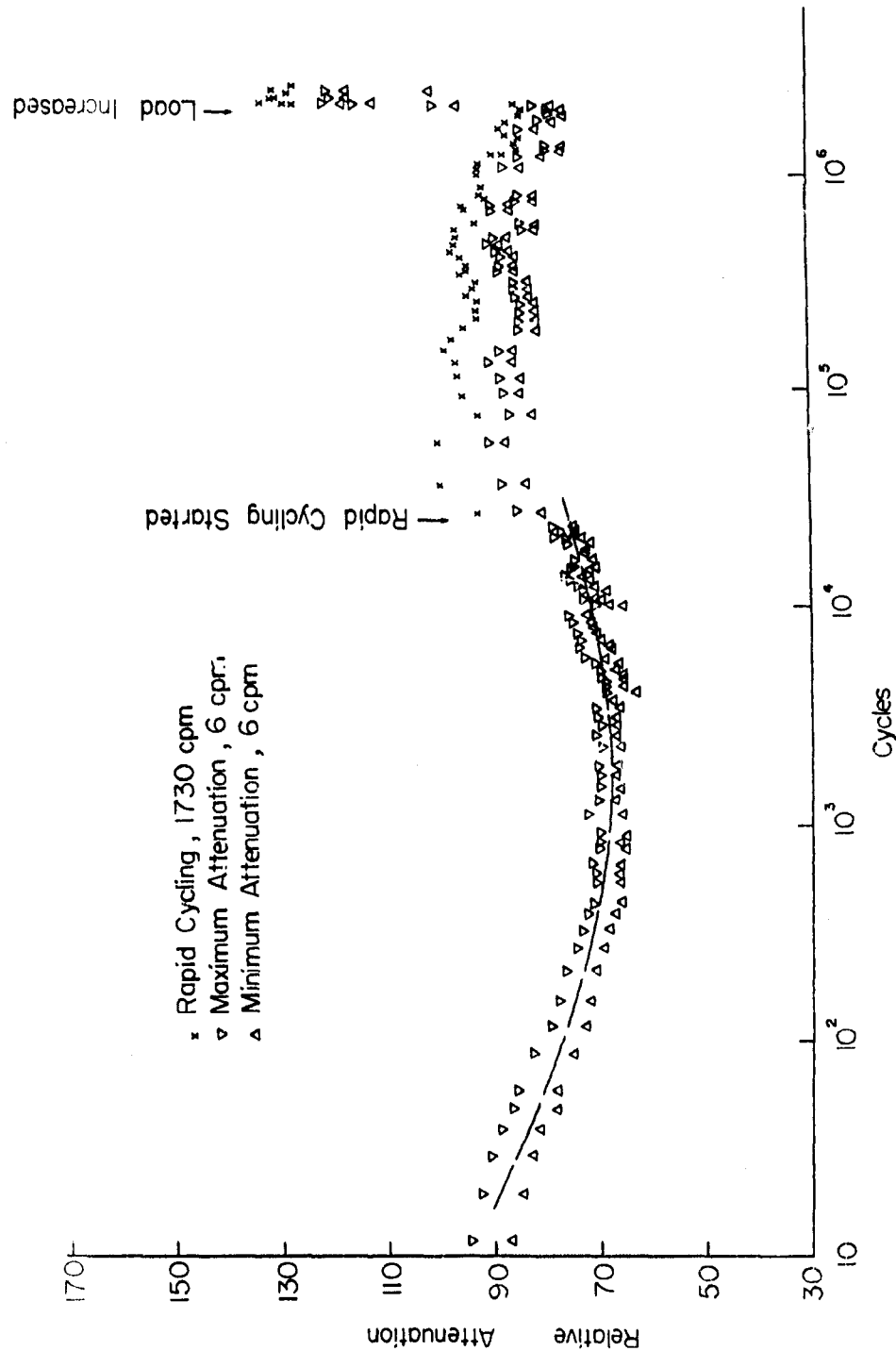


Figure 1
Maximum Attenuation, Minimum Attenuation (triangles) for slow (6 cycles/min) and average attenuation (x) for fast (1730 cycles/min) as a function of the number of stress cycles in tension and compression.

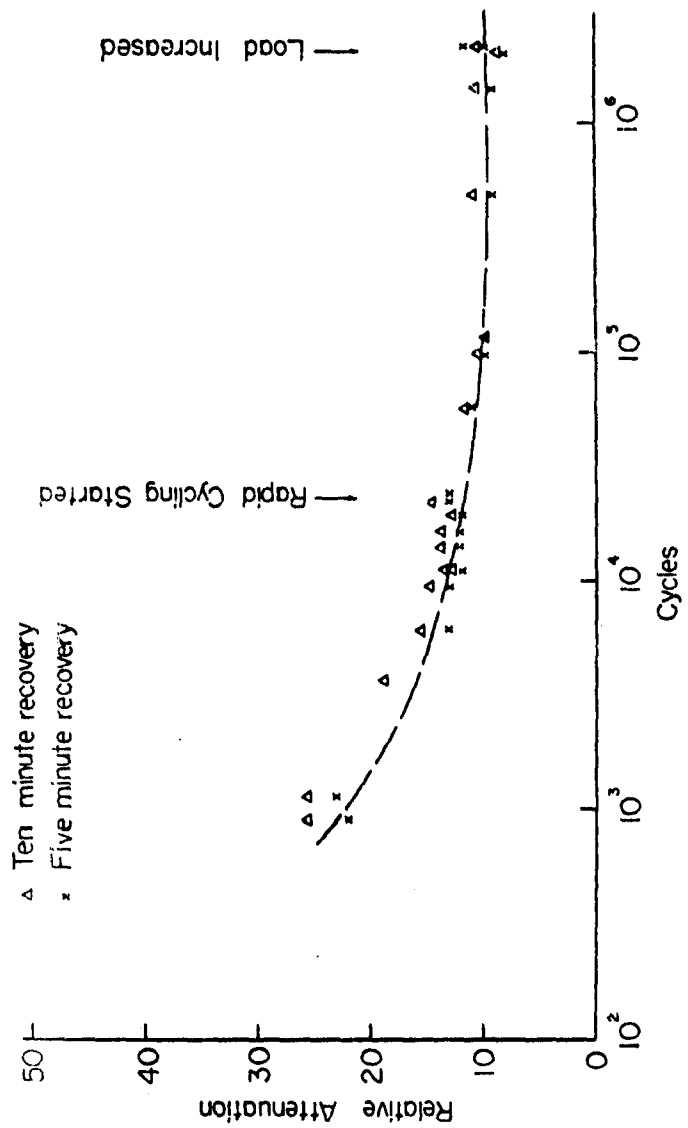


Figure 2
Attenuation recovery, for periods of five minutes and ten minutes after cycling is stopped,
as a function of number of stress cycles in tension and compression.

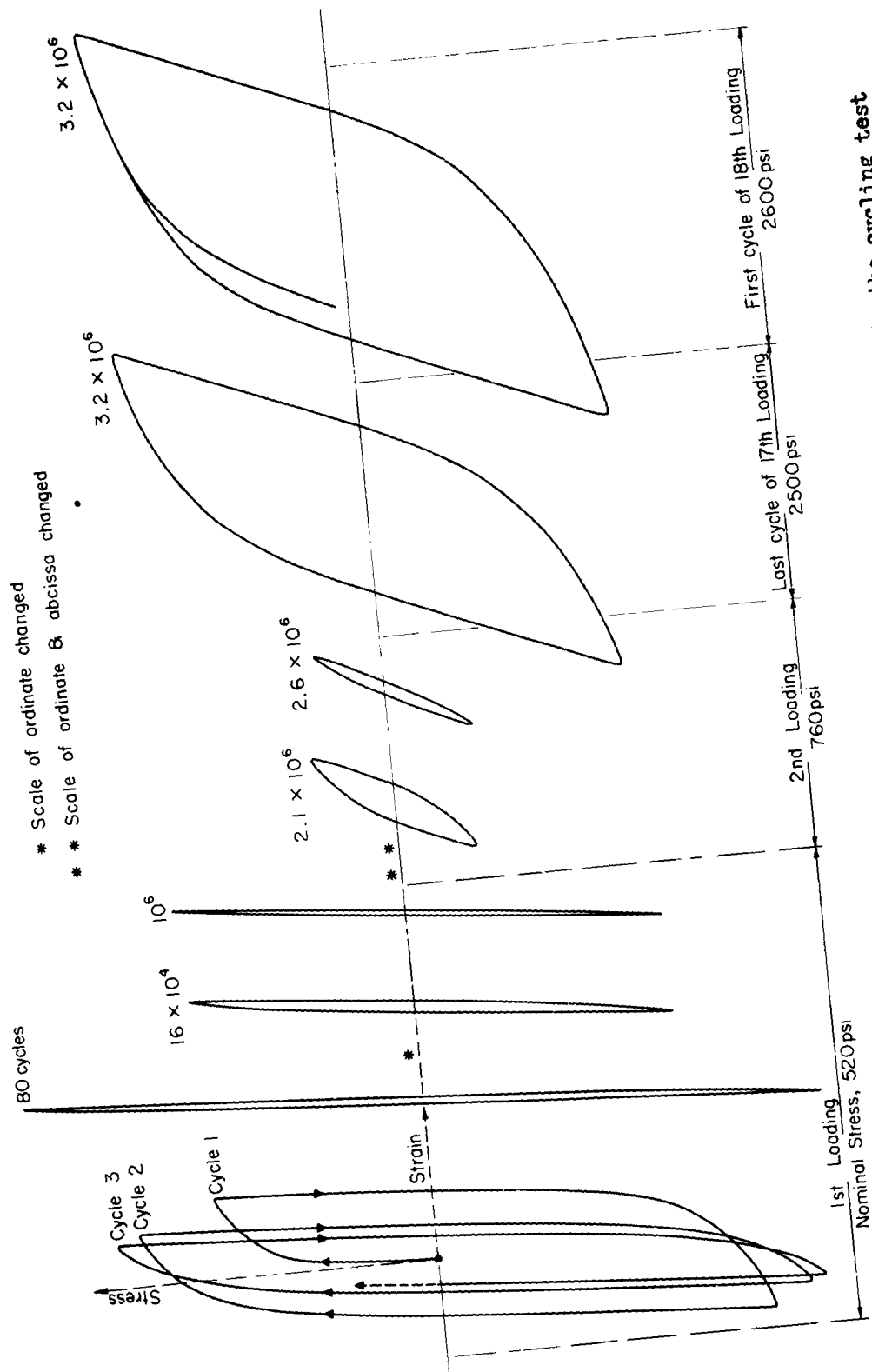


Figure 3
Representative stress-strain (hysteresis) loops at various stages in the cycling test
of a single crystal of aluminum.

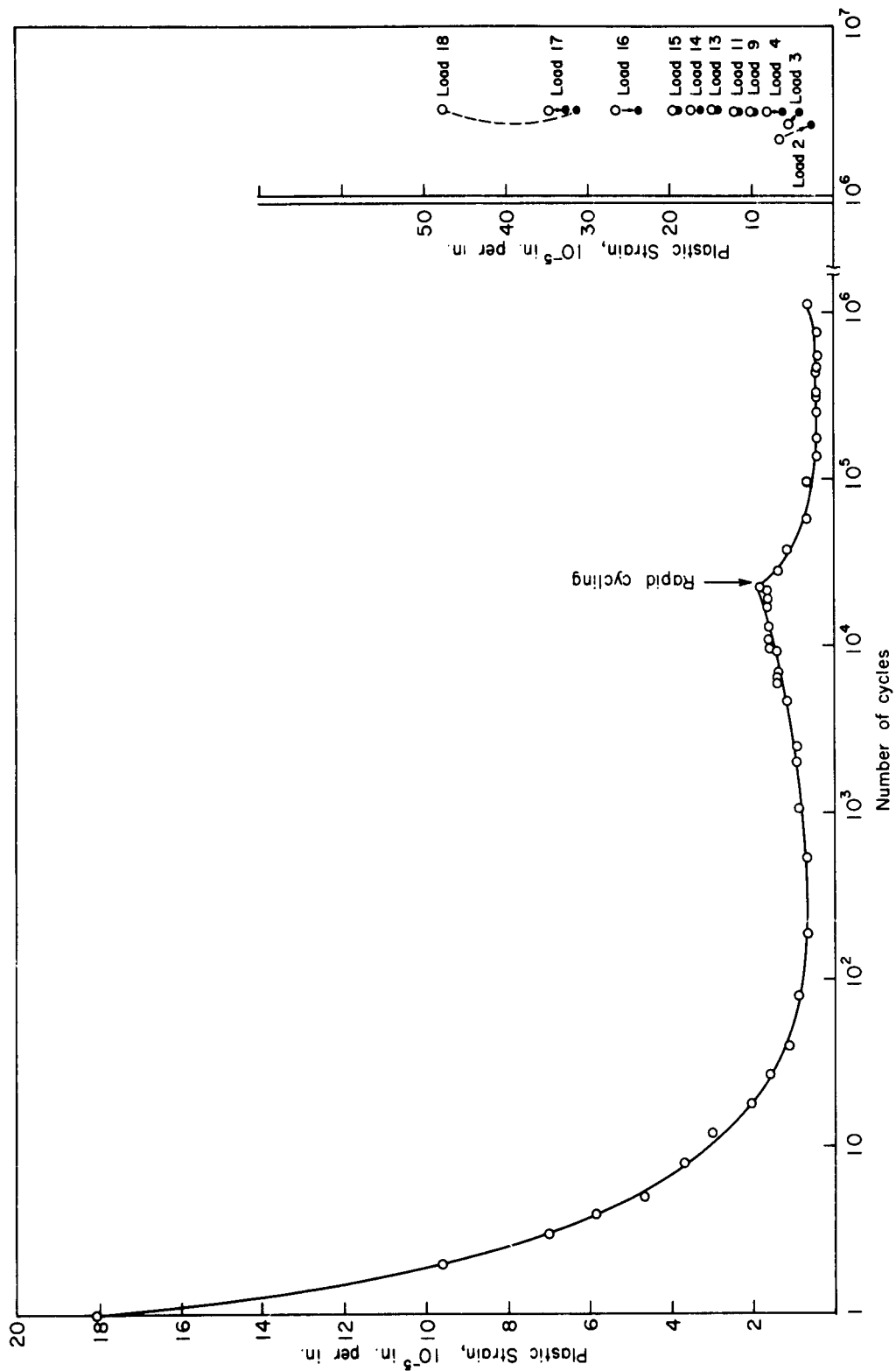


Figure 4
Width of hysteresis loop (Plastic Strain) versus number of cycles for single crystal of aluminum.

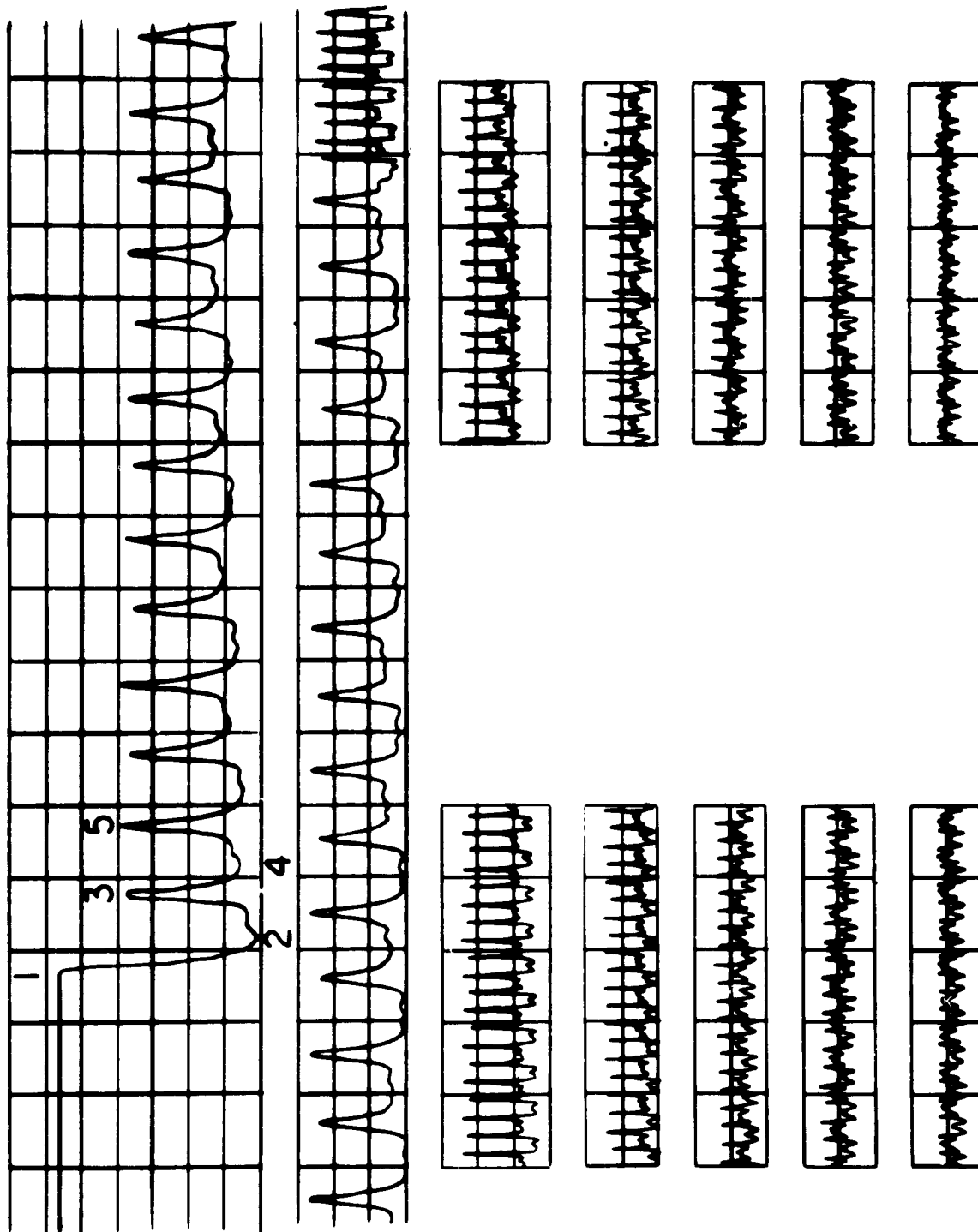


Figure 5
Sections taken from strip chart recording of automatic attenuation measurement unit
beginning with the start of cycling (top) and for about 100 cycles thereafter.

5. Automatic Recording Velocity Measurement Unit

The Automatic Recording Velocity Measurement Unit has been designed with two basic objectives in mind: (1) to be able to measure accurately and reliably the time between two repetitive (ultrasonic) signals (echoes) with a sensitivity of at least 1 nanosecond out of 100 μ sec (1 part in 10^5) and (2) to make the measurement available as a D. C. voltage capable of driving a recorder (either strip chart or X-Y) so that dynamic changes in time that cannot be measured manually will produce a permanent record that may later be examined in minute detail. Other important features are that the system be independent of variations in repetition rate and time jitter between the initiating pulse and the repetition rate generator.

The general block diagram for the device is shown in Figure 1. The exponentially decaying group of echoes are coupled from the R. F. mixer of the attenuation unit (at 60mc) into the matched 60 mc IF strips. The gain of each of these strips is approximately 80 db with a bandwidth of 5mc. The detected output (Figure 2a) of each IF strip is fed into a selector stage where all echoes except one are rejected. Since the echo selecting delays are in series (the delayed output of #1 triggers #2), the signal from selector #1 will always occur in time before the signal from selector #2. (If the delay time of Delay #2 could be made zero, then the signals could be made to coincide in time. In practice the delay of #2 is purposely restrained from capability of being zero.) The selected echoes (Figure 2b) are next amplified (Figure 2c) and shaped into triggers (Figure 2d). Shaped echo #1 simultaneously triggers delay #3 (Figure 3c) and the 1 μ sec marker generator gate (Figure 3a). The marker generator produces a 200 μ sec burst of 1 μ sec markers (Figure 3b) which are coupled into the marker selector. The output of delay #3 is also fed into the marker selector and makes it possible to select any marker from the 2nd through the 150th (Figure 3d). This selected marker is coupled into the monostable multivibrator section (Figure 4b) of the sawtooth generator (Figure 3d) as a "turn on" trigger (Figure 4a).

The "saw" rises at the rate of 50 volts per microsecond. Delay #3 is adjusted

so as to select the marker which occurs in time between 1 and 2 μ sec before the 2nd selected echo. The second selected echo (Figure 4c) is coupled into the sawtooth generator as a "turn off" trigger and terminates the "saw" at a voltage between 50 and 100 volts. As the time relationship between selected echo #1 and selected echo #2 changes, the amplitude to which the "saw" rises changes directly (Figure 5a,b,c,d). A peak detector converts the peak amplitude of the "saw" into a D. C. voltage which is measured in the balanced VTVM and made available to external recorders. The VTVM is a balanced device to allow the introduction of a 50 volt off-set voltage to compensate for the first microsecond of operation of the "saw". This allows measurements to zero on the "zero to one microsecond" vernier. This would be impossible to obtain on a linear basis if the sawtooth had to be measured back to a real zero voltage. This means then that delay #3 must be calibrated properly to account for this "lost" one microsecond. This is obviously readily accomplished. (A trivial limitation introduced by this method of operation is that the minimum time measurement capability is one microsecond rather than zero.) The total time between the two selected echoes is obtained by adding the corrected digital reading of delay #3 and the analog reading of the VTVM (or recorder). Under these conditions of operation of the analog portion of the readout, 50 volts represents 1 μ sec and the smallest time measurable on a conventional recorder will be 10 nanoseconds. By adjusting the offset voltage and changing the ratio of the dividing resistors in the VTVM by a ratio of 10:1 this smallest measurable time increment can be changed to 1 nanosecond. Theoretically this technique can be carried on for several more orders of magnitude of time readout sensitivity. In reality jitter problems and linearity of the "saw" make this difficult to do. It is hoped to be able to obtain 0.1 nanosecond sensitivity but experimental requirements will generally be satisfied with 1 nanosecond sensitivity.

Another section of the device which is necessary for satisfactory operation is

the AGC system. Each selected echo is fed into an AGC system which controls the gain of the appropriate IF amplifier and maintains the output of the IF amplifier constant within 1 db over a 40 db range of input signal. It is necessary to do this because the time measuring system is sensitive to the amplitude of signal fed into it. Since the amplitude of the two selected echoes would change different amounts under dynamic testing conditions, the AGC operation is required. (To make the application of AGC successful in this device it is also necessary to have IF amplifiers whose characteristics are not altered by the AGC voltage. We have succeeded in this requirement to the point where we can observe no change in center frequency or bandwidth over a 40 db range of gain control (Figure 6 a,b,c,d,e). Neither does an artificial change of 40 db in signal level to one IF amplifier produce a detectable change in measured time on the vernier readout).

The final result obtained with all these electronic amplifiers, delays, selectors, etc. is a device capable of measuring automatically with great sensitivity the time between two echoes. The measuring system is divorced from the basic sync circuits generating the signal so that jitter in the signal generating devices does not influence the measured value. Since both measured echoes are generated by the same initiating R. F. Pulse any change in shape or rise time in this pulse will not affect the final measured value. It should also be noted that the device is independent of the frequency at which the R. F. system is operating which means it is useful from approximately 10 mc to indefinitely high frequencies.

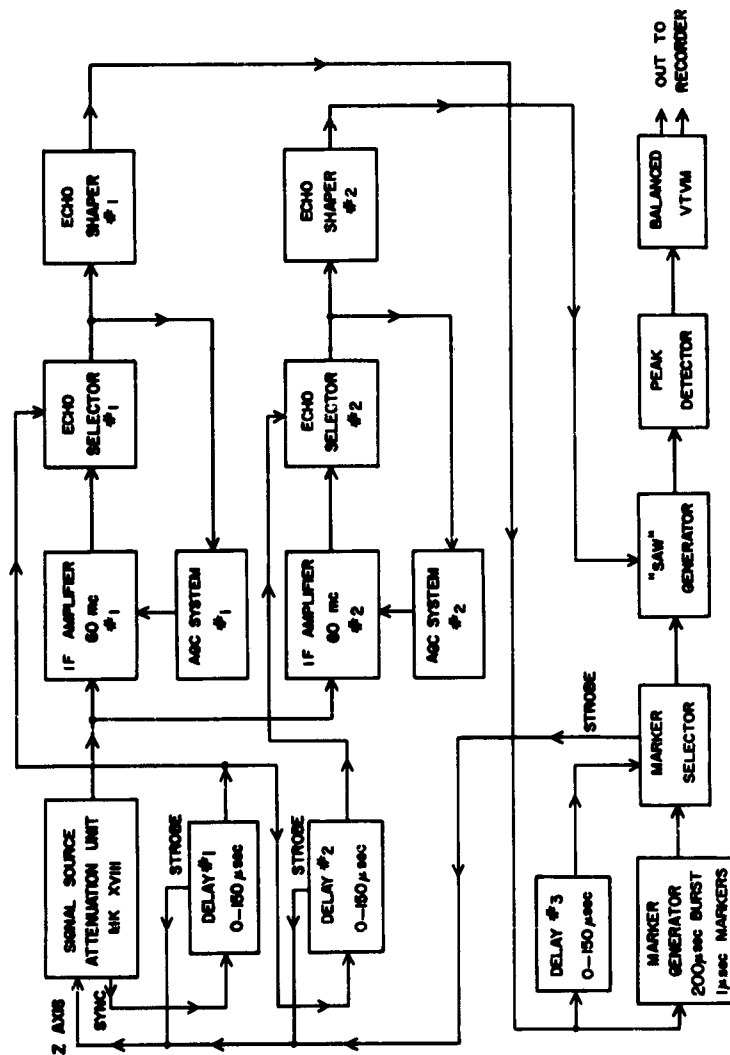


Figure 1
General Block Diagram - Automatic Recording Time Measurement Unit (ARTMU)



Figure 2

Echoes and shaped echo waveforms

- | | | | | |
|-----|--------|-----------------|-------|-------------|
| (a) | sweep: | 5 μ sec/cm; | sens: | 2 volts/cm |
| (b) | " | " | " | 1 volt/cm |
| (c) | " | " | " | 50 volts/cm |
| (d) | " | " | " | 25 volts/cm |

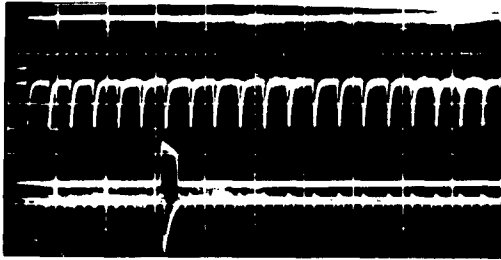


Figure 3

Marker generator and selected marker waveforms

- | | | | | |
|-----|--------|-----------------|-------|--------------|
| (a) | sweep: | 2 μ sec/cm; | sens: | 50 volts/cm |
| (b) | " | " | " | 50 volts/cm |
| (c) | " | " | " | 100 volts/cm |
| (d) | " | " | " | 20 volts/cm |

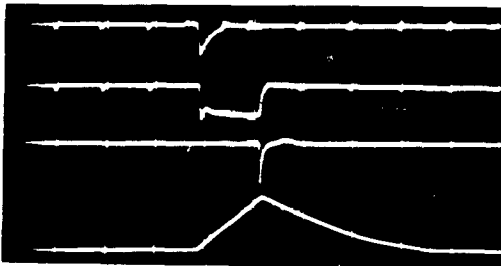


Figure 4

Sawtooth and sawtooth trigger waveforms

- | | | | | |
|-----|--------|-----------------|-------|-------------|
| (a) | sweep: | 1 μ sec/cm; | sens: | 20 volts/cm |
| (b) | " | " | " | 20 volts/cm |
| (c) | " | " | " | 50 volts/cm |
| (d) | " | " | " | 10 volts/cm |

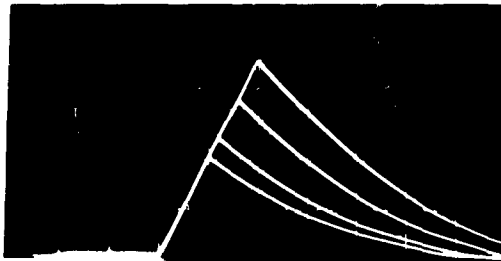


Figure 5

Sawtooth waveforms with various times

- | | | | | | |
|-----|--------|-----------------|-------|-------------|----------------------|
| (a) | sweep: | 1 μ sec/cm; | sens: | 25 volts/cm | analog time: 1000 ns |
| (b) | " | " | " | 25 volts/cm | analog time: 600 ns |
| (c) | " | " | " | 25 volts/cm | analog time: 200 ns |
| (d) | " | " | " | 25 volts/cm | analog time: 1000 ns |

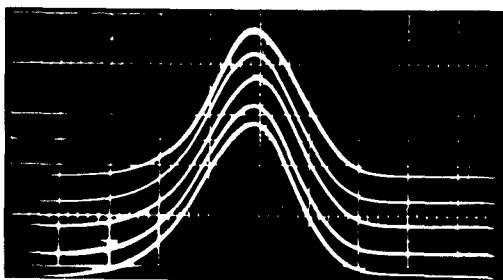


Figure 6

IF response curves at various sensitivities

- | | | | | |
|-----|--------|----------|----------|--------|
| (a) | sweep: | 4 mc/cm; | IF gains | max. |
| (b) | " | " | " | -10 db |
| (c) | " | " | " | -20 db |
| (d) | " | " | " | -30 db |
| (e) | " | " | " | -40 db |

REFERENCES

1. "Ultrasonic Attenuation and Velocity Data on Aluminum Single Crystals as a Function of Deformation and Orientation" A. Hikata, B. Chick, C. Elbaum and R. Truett, *Acta Metallurgica* 10, 423 (1962)
2. "Overdamped Resonance of Dislocations in Copper" A. V. Granato and R. Stern, *Acta Metallurgica* 10, 358 (1962)
3. "Dispersion of Elastic Waves in Sodium Chloride" A. Granato, J. deKlerk and R. Truett, *Phys. Rev.* 108, 895 (1957)
4. "Theory of Mechanical Damping Due to Dislocations" A. Granato and K. Lucke, *J. Appl. Phys.* 27, 583 (1956)
5. "Imperfections in Nearly Perfect Crystals" J. S. Koehler, p. 197 New York John Wiley and Sons Inc., 1952
6. "High Frequency Ultrasonic Stress Waves in Solids" Rohn Truett and Charles Elbaum, *Handbuch der Physik*, Volume XI Part 2
7. "Recovery of Damping and Modulus Changes Following Plastic Deformation" A. Granato, A. Hikata and K. Lucke, *Acta Metallurgica* 6 470 (1958)
8. "Über den Mechanismus der plastischen Deformation" A. W. Stepanow, *Z. Physik*, 81 560 (1933)
9. "Electrical Effects Associated With the Mechanical Deformation of Single Crystals of Alkali Halides" J. E. Caffyn and T. L. Goodfellow, *Nature*, 176 878 (1955)
10. "Deformation-Induced Charge Flow in NaCl Crystals" D. B. Fischbach and A. S. Nowick, *Phys. Rev.* 99, 1333, (1955)
11. "Some Transient Electrical Effects of Plastic Deformation in NaCl Crystals" D. B. Fischbach and A. S. Nowick, *J. Phys. Chem. Solids* 5 302, (1958)
12. "Influence of Plastic Flow on the Electrical and Photographic Properties of the Alkali Halide Crystals" F. Seitz, *Phys. Rev.* 80 239, (1950)
13. "Conduction in Polar Crystals" N. F. Mott and N. J. Littleton, *Trans. Faraday Soc.* 34 485, (1938)
14. "Kinetic Theory of Liquids" J. Frenkel, Oxford (Clarendon Press), (1946)
15. "Space-Charge Layer and Distribution of Lattice Defects at the Surface of Ionic Crystals" K. Lehovec, *J. Chem. Phys.*, 21 1123, (1953)
16. "Charged Dislocations and the Strength of Ionic Crystals" J. D. Eshelby, C. W. A. Newey, P. L. Pratt and A. B. Lidiard, *Phil. Mag.* 3 75, (1958)

17. "Electrical Effects During Cyclic Stressing of Sodium Chloride" S. Amelinckx, J. Vennik and G. Remaut, J. Phys. Chem. Solids 11 170, (1959)
18. "Further Observations Concerning Electrical Effects During Cyclic Stressing of Alkali Halide Single Crystals" G. Remaut, J. Vennik and S. Amelinckx, J. Phys. Chem. Solids 16 158, (1960)
19. "Charged Dislocations in Lithium Fluoride" R. L. Sproull, Phil. Mag. 5 815, (1960)
20. "Observations on an Electrical Effect Obtained During Deformation of Sodium Chloride Crystals" G. Remaut and J. Vennik, Phil. Mag. 6 1, (1961)
21. "Observations on Charged Dislocations in Ionic Crystals" J. Vennik, G. Remaut and W. Dekeyser, Phil. Mag. 6 997, (1961)
22. "Charge Effects During Inhomogeneous Deformation of Rocksalt" F. Rueda and W. Dekeyser, Phil. Mag. 6 359, (1961)
23. "Charged Dislocations in Ionic Crystals" F. Rueda and W. Dekeyser, J. Appl. Phys. 32 1799, (1961)
24. "Charged Dislocations in Pure and Doped Rocksalt Single Crystals" F. Rueda and W. Dekeyser, Acta Metallurgica 11 35, (1963)
25. "The Movement of Charged Dislocations in Sodium Chloride" J. E. Caffyn and T. L. Goodfellow, Proc. Phys. Soc. 79 1285, (1962)
26. "Electrical Effects Produced by Plastic Deformation in Sodium Chloride Crystals" J. E. Caffyn and T. L. Goodfellow, Phil. Mag. 7 1257, (1962)
27. "Sign of Charged Dislocations in NaCl" J. E. Caffyn and T. L. Goodfellow J. Appl. Phys. 33 2567, (1962)
28. "Association Energy of Vacancies and Impurities With Edge Dislocations in NaCl" F. Bassani and R. Thomson, Phys. Rev. 102 1264, (1956)
29. "Calculation of the Charge on Dislocations in NaCl", G. Remaut phys. stat. sol. 2 576, (1962)
30. "Charged Dislocations in Ionic Crystals", J. S. Koehler, D. Langreth and B. von Turkovich, Phys. Rev. 128 573, (1962)
31. "Dislocation Damping in Sodium Chloride", A. Hikata, B. Chick, C. Elbaum and R. Truett J. Appl. Phys. Letters, Jan. 1963

Aeronautical Systems Division, Dir/Materials & Processes, Metals and Ceramics Lab, Wright-Patterson AFB, Ohio
Rpt No. ASD-TDR-62-186, Pt. II ULTRASONIC METHODS IN THE STUDY OF FATIGUE AND DEFORMATION IN SINGLE CRYSTALS, Final report, Feb 63. 76p., incl illus., 31 refs.

Unclassified Report

Ultrasonic methods for studying defect formation and motion in connection with deformation and stress cycling experiments in aluminum and sodium chloride single crystals is the subject of this report. Large single crystals of sodium chloride, deformed in tension, were measured similarly to aluminum for the purpose of comparing the dislocation damping and recovery effects in an ionic crystal with those in a metal. Also there was significant

1. Deformation Recovery
2. Ionic Crystals
3. Stress-Strain
4. Aluminum Crystals
5. Sodium Chloride Crystals

I. AFSC Project 7360

Task 736002

II. Contract No.

AF 33(657)-8324

III. Brown University

IV. Providence, R. I.

V. Chick, et al.

VI. Avail fr OTS

VI. In ASTIA collection

Aeronautical Systems Division, Dir/Materials & Processes, Metals and Ceramics Lab, Wright-Patterson AFB, Ohio
Rpt No. ASD-TDR-62-186, Pt. II ULTRASONIC METHODS IN THE STUDY OF FATIGUE AND DEFORMATION IN SINGLE CRYSTALS, Final report, Feb 63. 76p., incl illus., 31 refs.

Unclassified Report

Ultrasonic methods for studying defect formation and motion in connection with deformation and stress cycling experiments in aluminum and sodium chloride single crystals is the subject of this report. Large single crystals of sodium chloride, deformed in tension, were measured similarly to aluminum for the purpose of comparing the dislocation damping and recovery effects in an ionic crystal with those in a metal. Also there was significant

1. Deformation Recovery
2. Ionic Crystals
3. Stress-Strain
4. Aluminum Crystals
5. Sodium Chloride Crystals

I. AGSC Project 7306

Task 736002

II. Contract No.

AF 33(657)-8324

III. Brown University

IV. Providence, R. I.

V. Chick, et al.

VI. Avail fr OTS

VI. In ASTIA collection

Information from electrical conductivity measurements made concurrently with attenuation and velocity measurements. Comparison of Al single crystals at 195°K with room temperature resulted in an interesting "threshold effect." Al single crystals were also stress cycled in tension and compression at levels much higher relative to yield stress and breaking stress than polycrystalline samples, and at the same time the stress level can be raised in steps during cycling to 1/2-2 times the stress required to break the single crystal sample. The trial model automatic recording time echo (or velocity) measurement unit test gave no change in center frequency of bandwidth over a 40db range of gain control nor an artificial change of 40db in signal level to produce a detectable change in measured time

Information from electrical conductivity measurements made concurrently with attenuation and velocity measurements. Comparison of Al single crystals at 195°K with room temperature resulted in an interesting "threshold effect." Al single crystals were also stress cycled in tension and compression at levels much higher relative to yield stress and breaking stress than polycrystalline samples, and at the same time the stress level can be raised in steps during cycling to 1/2-2 times the stress required to break the single crystal sample. The trial model automatic recording time echo (or velocity) measurement unit test gave no change in center frequency of bandwidth over a 40db range of gain control nor an artificial change of 40db in signal level to produce a detectable change in measured time.